AD NUMBER

AD478559

LIMITATION CHANGES

TO:

Approved for public release; distribution is unlimited.

FROM:

**Distribution authorized to U.S. Gov't. agencies and their contractors;
Administrative/Operational Use; MAY 1965. Other requests shall be referred to Frankford Arsenal, Philadelphia, PA.**

AUTHORITY

USAFA ltr, 7 Jul 1971

478559

TECHNIK

TECHNIK INCORPORATED

SUMMARY REPORT

ANALYSIS OF

ADVANCED MECHANICAL TIME FUZE COMPONENTS

By: Technik Incorporated
50 Jericho Turnpike
Jericho, New York

TR #65-9
May 1965

For: Frankford Arsenal
Philadelphia, Pa.

Contract No. DA-30-069-AMC-17(A)

CONTENTS

CONTENTS (continued)

NOMENCLATURE

a = contact radius

b = width of cross section

c = constant of coil geometry ($2\pi c$ = coil spacing)

g = acceleration due to gravity

h = depth of cross section

i = numerical index indicating particular coil, $1 \leq i \leq n$ (subscript)

j = numerical index indicating iteration cycle (superscript)

k = spring constant

l = length

m = mass of spring per unit length

n = number of coils of spring (or number of g's)

p = pressure, q = pressure

r = spring radius

s = coordinate of length measured along spring coil

u = radial deformation of spring

x = variable numerical index

A = cross sectional area of spring

C = constant of integration

E = modulus of elasticity

F = force, F_o = preload

I = moment of inertia of spring section

K = constants, defined as used, in text

M = spring bending moment

M_i = value of M at attachment to barrel

M_{max} = maximum value of M (at attachment to arbor)

P = force

R = ratio of any coil radius to radius of last (largest) coil = $\frac{R_i}{R_n}$

$S_i^{(j)} = [1 - (\frac{\omega^{(j-1)}}{\omega^{(j)}})^2 (\frac{r_i^{(j-1)}}{r_i^{(j)}})^2]$

$\alpha = S_i^{(j)} / S_n^{(j)}$

T = torque at spring arbor

T_{max} = maximum linear value of T (occurs at $\varphi = \varphi_{max}$)

U = strain energy of spring

W = work done in coil deformation

α = angular measurement following spiral of coils

δ = linear deformation

$\delta\alpha$ = change in angle

ΔR = change in radius

ϵ = eccentricity of spiral

π = 3.1416

Π = potential function = $U - W$

σ = stress

σ_y = yield stress

ρ = radius of curvature

μ = coefficient of friction

ν = poisson's ratio

τ = shear stress

φ = angle of spring wind-up from position at rest in barrel

φ_L = point, φ, at which linear action initiates (all coils are "free")

φ_{max} = point, φ, at which linear action ceases (spring begins to extend)

ω = spin rate

1. INTRODUCTION

This report will serve to summarize the analysis, and the conclusions drawn therefrom, in compliance with the requirements of contract #DA-30-069-AMC-17(A). A summary of these conclusions will be found in section 2 of this report, and the full analysis is reported in sections 3 to 6. The subjects of this analysis are somewhat varied in view of the nature of the "Scope" of the contract, which calls for analysis in problem areas of more or less independent content. The general areas covered are related to the effects of the dynamic projectile environment upon specific fuze components:

(a) Spiral Motor Springs

(b) Pivot and Journal Friction

(c) Torsion Hair Springs

(d) Beam Hair Springs

Thus, the performance characteristics and various specific aspects of the behavior of these components in a spin or setback environment will be the subject of the following discussion.

The initial analysis undertaken pursuant to contract #DA-30-069-AMC-17(A) was concerned with the analysis of spiral motor springs. This analysis had, as its objective, the determination of the effects of projectile spin upon the torque yield of the motor spring.

It was determined that in order to obtain physically meaningful results, the non-spinning or "static" spring must be fully understood. At the time, the body of literature which dealt with spiral springs considered only those springs unconstrained radially by an outer barrel. A great deal of empirical evidence

was available which supported the view that the existing analytical approaches were inapplicable to "real" springs.

Thus the "static" analysis was undertaken to determine the character of the relationship between arbor torque and the physical parameters of the spring. This was determined, yielding the equation governing the "torque-turn" characteristic within the region of interest. This equation, in addition to being of great utility and interest, forms the basis for comparison in evaluating the spin effects.

The next step in the analysis was facilitated by dividing the spin effect into its simplest constituents. i.e., axisymmetric extensional deformation and axisymmetric bending deformation. The effect of these modes of deformation upon the torque output at the arbor is described in detail in section 3 of this report, along with the "static" torque-turn characteristic. In this same section the possibility of the incidence of greatly eccentric deformations was introduced.

The question of eccentric deformation received preliminary analytical and experimental study; as reported in section 3. This mode of deformation was not foreseen at the outset of the investigation, nor was the possible extent of its effects. These effects are indicated, on an order of magnitude basis.

Investigations of pivot friction under the influence of high centrifugal loading due to projectile spin are indicated in section 4, following the discussion of motor spring eccentricity. Calculations are performed for the fully elastic condition of the pivot and pivot seat. It is noted that under ordinary conditions, plastic action and accelerated wear may easily become important considerations.

The beam hair-spring problems associated with this contract are included in section 5.

Preliminary investigation of the torsion spring-critical speed problem is indicated in section 6. It is found that, for particular cases of spring geometry, the various modes of critical speed may be related to the torsional frequency parameters of the escapement. Similar relationships may be established for other configurations of interest.

2. CONCLUSIONS

2.1 SPIRAL MOTOR SPRING

The various stages of this investigation are listed below, for reference:

(a) Study of torque-turn relationship for non-spinning spiral motor spring

  (1) Relationship in linear region

  (2) Maximum torque (utilizing "limit plastic" effects)

(b) Axi-symmetric effects of spin environment

  (1) Effects of extensional deformations

  (2) Effects of bending deformations

(c) Non-axi-symmetric effects of spin environment

  (1) Sources of spiral eccentricity

  (2) Eccentric effects.

Of the above listed topics, the non-spinning spring characteristics have been fully explored, as indicated in section 3.2. Only in the event that it is found desirable to use the non-linear region of the torque-turn characteristic, would it be necessary to pursue the investigation of the non-spinning spring further than has been presently completed.

Axi-symmetric effects of the spin environment are presented in section 3.3. These effects are discussed in great detail, and the analytical tools are developed for their determination in any given case. Further work in this area would be concerned with the establishment of the relationship between torque, deformation and spring parameters; and, therefore, of torque-spin-sensitivity.

The incidence of non-axi-symmetric deformations and the torque perturbations resulting therefrom, is pointed out in section 3.3.2. As is discussed there, analysis of this phenomenon is, in many respects, an extension of the axi-symmetric analysis. It is true, however, that this extension is not minor in execution, although the basic concept of approach follows that already developed for the axi-symmetric case.

Technik has found that in addition to axi-symmetric effects investigated within the scope of this contract the torque variations due to eccentric effects could be a dominant controlling factor in the proper utilization of spiral springs in fuze design. The presence of these eccentric effects was first noticed from empirical evidence and then verified analytically. It was found that the existence of this eccentricity is intrinsically tied to the spiral spring geometry. The magnitude of the associated torque effects is dependent upon the parameters of the spring design and the spin environment. However, the specific relationship between eccentric behavior and physical parameters, has <u>not</u> yet been established.

Extensive deformation of this sort would result in a major perturbation upon the torque-turn characteristic, above that induced by the axi-symmetric modes of deformation. At the present stage of Technik's analysis, the extension to eccentric deformation is a natural next step. As such, it involves an advance of the current state-of-the-art (as presented in section 3), which should be built upon the foundation of the current level of knowledge. Technik's present level of experience with this analysis will prove an invaluable asset in continuing the investigation of <u>all</u> the ramifications of problems associated with spiral motor springs.

A summary of the analytical results of the spiral spring analysis will be found in section 3.4.

2.2 OTHER PROBLEMS

In addition to the major effort expended on the analysis of spiral motor springs, during the course of this contract several other independent problems received Technik's attention as per the directions of the technical supervisor and the provisions of the contract "Scope". The results of these investigations will be found in the respective sections devoted to the analysis (4,5 and 6).

Briefly, these sections represent first-order analyses of torque losses in pivots and journal bearings under high centrifugal loading, of critical speeds in a torsional hair spring and of setback and fabrication technique effects on beam hair springs.

In the section on pivot and journal friction, it is found that, in addition to conventional friction considerations, the high loads associated with high projectile spin rates may cause plastic deformation effects (brinelling). This type of deformation would influence the nominal elastic torque characteristics of the bearing and may lead to a situation designated as accelerated wear, where the material is capable of shearing under the frictional loading developed.

In section 5, it is shown that for the normal range of beam hair spring dimensions considered, resistance to setback loading is limited by the onset of plastic action rather than by beam buckling. Thus the indicated design procedure is to increase the plastic carrying capacity of the spring cross-section with only secondary regard to the elastic stability of the beam. In addition, the effects of a wedge retainer upon beam hair spring deformation are shown

to be extensive over the length of the spring. Thus, this should be reconsidered if it is to be a method of fabrication.

The final section indicates the unique relationship that exists between all the torsion hair spring parameters. The same parameters determine critical speed and natural frequency, thus knowledge of one may be used to indicate the other, without the necessity of direct appeal to all implied parameters.

3. SPIRAL MOTOR SPRINGS

3.1. INTRODUCTION

This report will summarize Technik's analysis, to date, with respect to the behavior and deformation of spiral motor springs in a spin environment. The axis of spin is taken perpendicular to the plane of the spring, as is conventional in mechanical time fuse practice; with the arbor axis colinear with the projectile spin axis. This analysis is provided for under contract #DA-30-069-AMC-17(A).

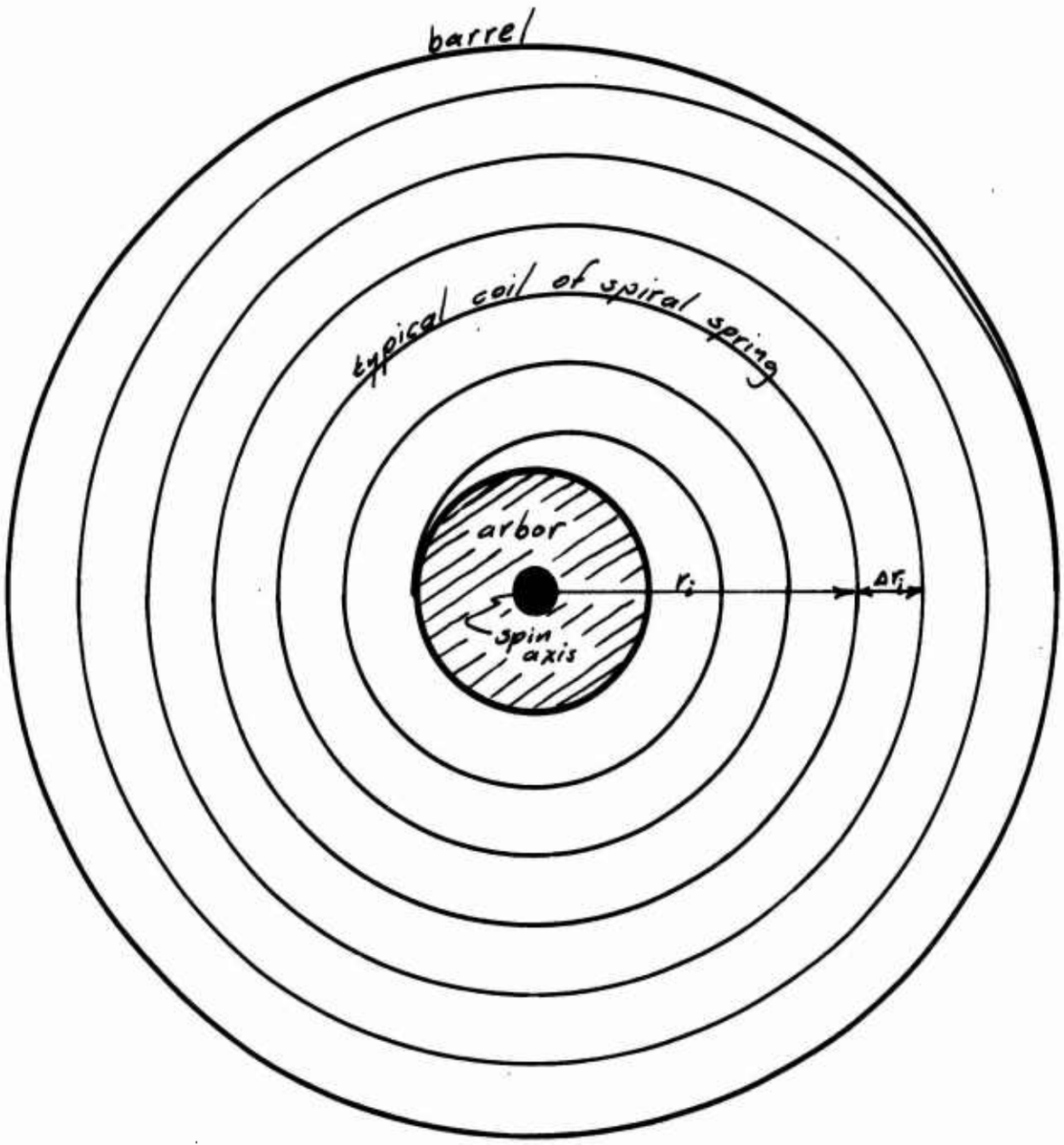

In order to fully understand motor spring characteristics in a spin environment, it is first necessary to understand these same characteristics in the non-spinning condition. It appears that even non-dynamic spiral spring theory has not previously been brought into agreement with the type of empirical data which is observed by spring makers and users.

Thus the program has been divided into phases of investigation dealing separately with (1) non-spinning and (2) spinning environments. It was found that the "spin analysis" could advantageously be further sub-divided into so-called "membrane" and "bending" solutions representing extensional spring deformation and bending deformation in the plane of the spring, respectively.

The bending solution, which will be found to present the greatest phenomenalogical complexity, may be examined from the viewpoint of a superposition of eccentric effects upon an (almost) axially symmetric solution. The coupling of these two separate effects, which in combination with the other analytical results of this program represents the complete solution to the spinning motor spring problem. This report emphasizes the various aspects of the symmetrical mode of deformation of the motor spring; limiting discussion of the eccentric effect to its preliminary aspects. The importance of this latter mode of deformation was only recently determined during the course of experimentation. Later work will explore it more fully.

3.2. TORQUE-TURN CHARACTERISTICS OF NON-SPINNING MOTOR SPRINGS

3.2.1 GENERAL REMARKS

Study of Frankford Arsenal drawings, photographs and experimental torque-turn characteristics, which are presented in the following figure, indicates the following general conclusions regarding the non-spinning spring:

(a) Experimental Torque-Turn characteristics indicate a discrepancy between wind-up and run-down curves.

(b) The area between these curves is indicative of the energy lost to the system, i.e., the excess of energy required to wind the spring over that released by the spring in unwinding.

(c) Spring energy losses during the period of interest (the run-down cycle) are indicated by the area between the "ideal" run-down characteristic and curve; which ia a "mean" between the wind-up and the run-down.

(d) The basic shape of the characteristics are often overlaid by cyclic perturbations corresponding to local disturbances in the geometry of the spring-barrel-arbor combination; indicative of additional energy losses due to friction between local points in contact.

(e) The torque turn characteristic normally changes its character at some point in the wind-up or unwinding cycle, between a linear and a non-linear relationship.

(f) There is another basic change in the shape of the characteristic at

the maximum number of turns (i.e., when the spring is wound "solid"), at which point the slope of the characteristic changes radically ($\frac{dT}{d\varphi} \rightarrow$ very large).

The element of area on the preceding curve, which is $T d\varphi$, represents the elemental energy, dE. Thus the single cross-hatched areas shown between the perturbed characteristic shape and the non-perturbed wind-up or run-down characteristics is a measure of energy loss due to friction imposed by local effects (interference between eccentric portions of spring). Likewise the energy loss between wind-up and run down is represented by the overall area between the two curves, whereas the available energy is that (double cross-hatched) enclosed by the run-down curve.

In the following treatment, the effects of friction are not considered. Those effects, which are of great importance in their own right, are not first-order considerations in the present problem of the spinning motor spring. Further, this section will be limited to theoretical derivations of the necessary equations.

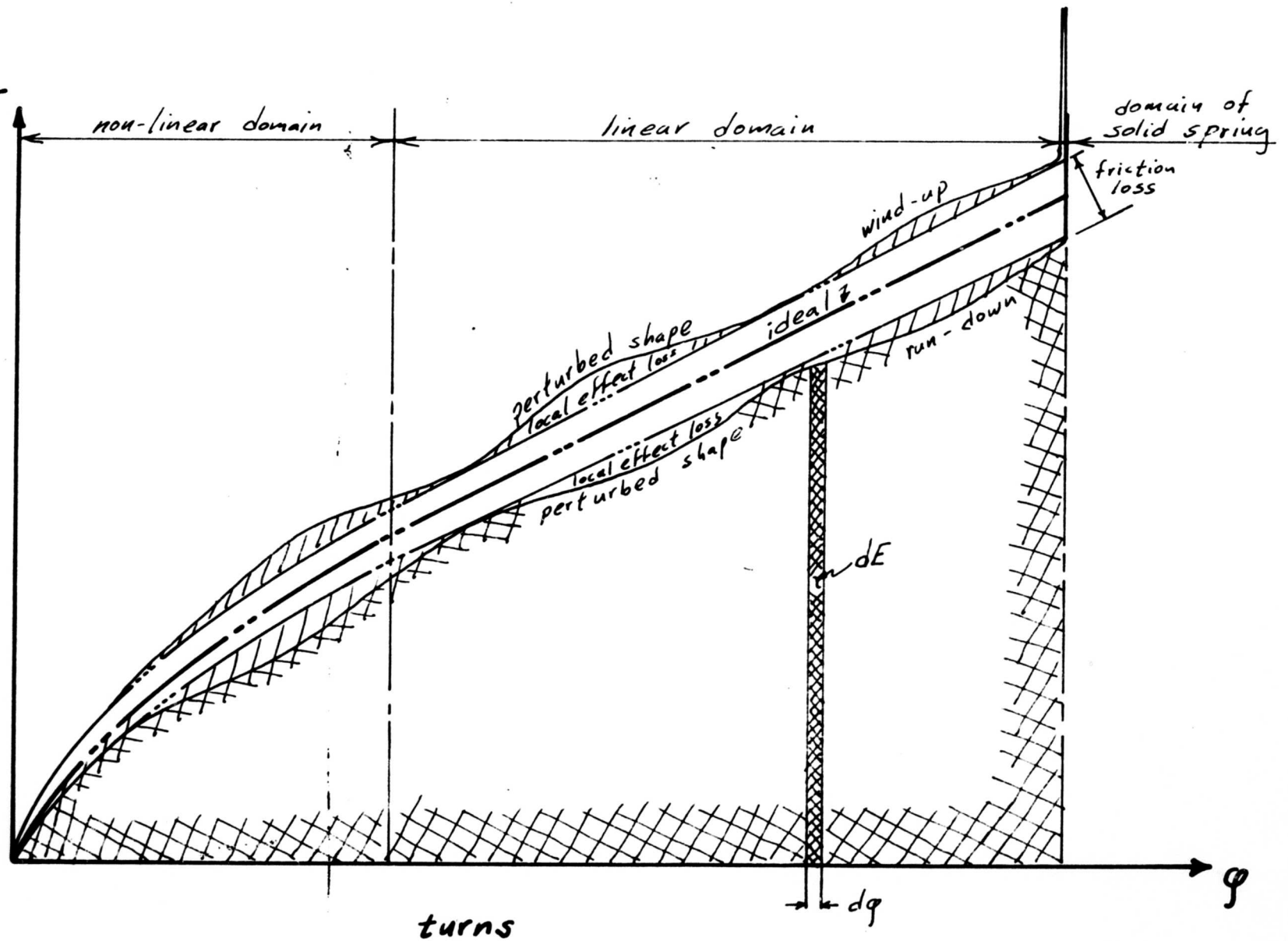
T
non-linear domain
linear domain
domain of solid spring
friction loss
wind-up
perturbed shape
local effect loss
ideal
run-down
local effect loss
perturbed shape
dE
dφ
φ
torque
turns

3.2.2 DETERMINATION OF TORQUE-TURN CHARACTERISTICS IN LINEAR RANGE

Many references may be found which deal with the spiral spring in the condition where adjacent coils are not in contact. (e.g., Chapter 27 of Wahl's "Mechanical Springs") The relationships to be found in these references take the form:

$$T = \frac{EI}{l} K\varphi$$

where T = torque delivered to arbor by spiral spring

EI = bending stiffness of spring section

l = spring length

φ = number of deflected turns undergone by spring

K = constant depending on prescribed boundary condition at outer boundary: fixed end $\Rightarrow 1 \leq K \lesssim 1.25 \Leftarrow$ pinned end

The problem which arises in the application of this relationship is generated by the incompatability, in practice, of the definition of φ with the requirement for non-contact. i.e., when $0 \leq \varphi \leq \varphi_i$ some coils are in contact. Thus, in the normal course of events the important position of zero torque occurs precisely in that range of values of φ where the clasical solution does not apply.

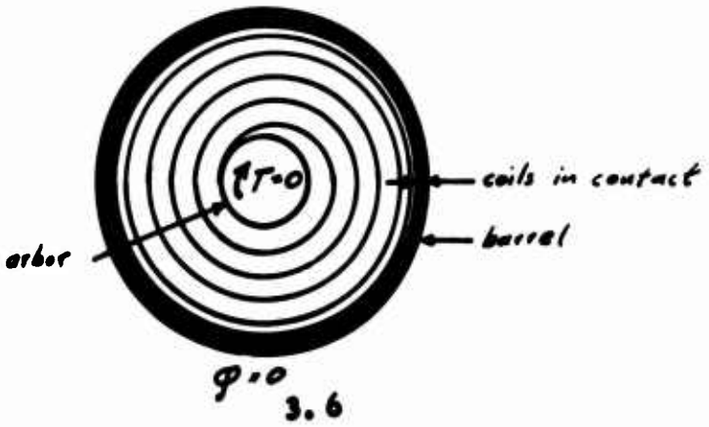

3.6

Thus, in the barrel, the spring delivers zero torque at some non-zero number of turns; which is beyond the validity of the classical solutions.

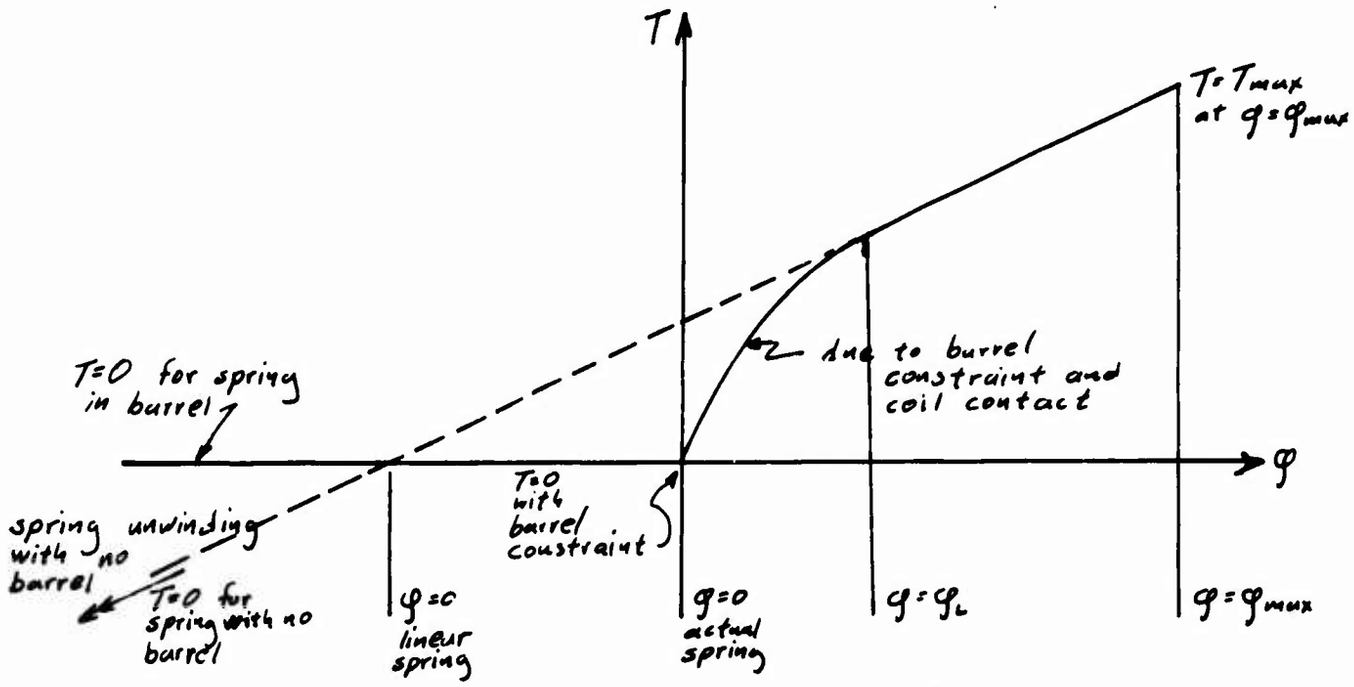

In recognition of the ambiguity of the location of the point $\varphi = 0$, due to the barrel constraint and the resulting non-linearity of the solution for $\varphi < \varphi_L$, the linear solution may be used only to find the slope ($\frac{dT}{d\varphi}$) for values of $\varphi > \varphi_L$. Further, it is sufficient to arrive at the proper solution in this linear range, at this time, since the spring is always used in the range $\varphi > \varphi_L$ range for time fuze applications.

Given the slope, within the range of interest (i.e., $\frac{dT}{d\varphi} = K\frac{EI}{l}$ one may integrate to find:

$$T = \frac{EI}{l} K \varphi + C .$$

which differs from the conventional expression only by the constant, C. Any boundary condition can determine the value of C, but since the zero boundary condition is submerged in the non-linear range of the solution, the

boundary condition at φ_{max} will be utilized.

Thus, using the notation $T = T_{max}$ at $\varphi = \varphi_{max}$, the full expression for the torque-turn characteristic is found to be:

$$T = T_{max} - \frac{EI}{l} K (\varphi_{max} - \varphi)$$

In the above expression, which is valid for the linear regions of the characteristic, T_{max} may be supplied from experimental measurements, or analytically as shall be discussed in the following section. It is to be noted that the limitations imposed by the theoretical assumptions do not seem to be important limitations in the correlation between experiments and these these theoretical results.

3.2.3 DETERMINATION OF MAXIMUM TORQUE (T_{max})

3.2.3.1. Total Spring Torque

A free body diagram of the spring and of the arbor will illustrate the relation between the moment, $M_{\varphi max}$, and the torque, T_{max}. Assuming a simply supported end at the barrel:

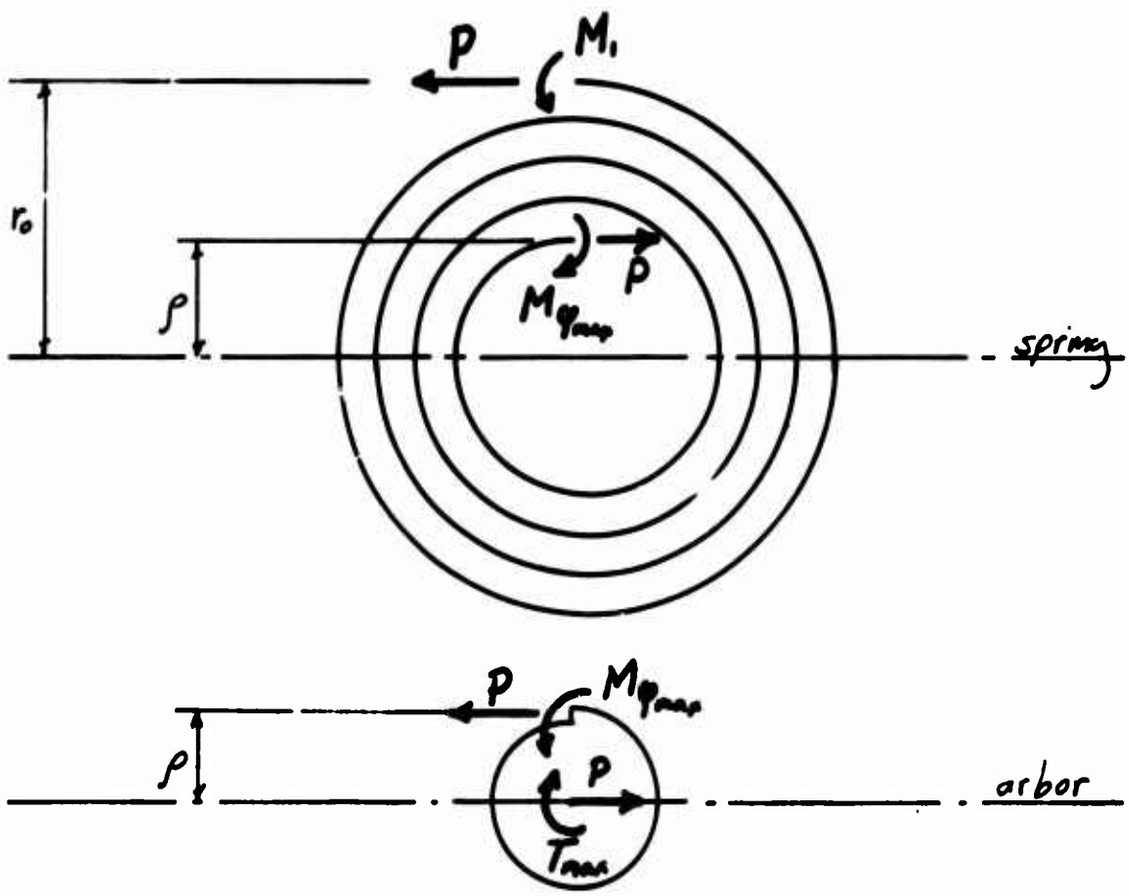

Equilibrium equations result in

$$T_{max} = P r_o + M_1$$
$$T_{max} = P \rho + M_{\varphi max}$$

or combining through the elimination of P, there results

$$T_{max} = \frac{M_\varphi - M_1 \left(\frac{\rho}{r_o}\right)}{1 - \left(\frac{\rho}{r_o}\right)}$$

For the case where the end at the barrel is pinned $M_1 = 0$ and

$$T_{max} = \frac{M_\varphi}{1 - \left(\frac{\rho}{r_o}\right)}$$

Further it can be shown for the <u>elastic</u> case with a fixed end at the barrel that $P = 0$ and

$$\therefore T_{max} = M_\varphi$$

In general we can write

$$T_{max} = K_1 M_\varphi$$

where for the elastic case

$$K_1 = \left\{ \begin{array}{ll} 1 & \Rightarrow \text{fixed} \\ \frac{1}{1 - \frac{\rho}{r_o}} & \Rightarrow \text{pinned} \end{array} \right\} \text{end}$$

Further, since the spring unloads and reloads elastically, even when it has received a prior plastic deformation to achieve its form from the flat stock, this value of K_1 will hold in general. Cases other than pinned or fixed end can be considered separately but we can assume they will be within the range indicated above.

3.2.3.2 Elastic Case

The torque, T, which can be exerted by the spring, in its most general position, is determined from that moment associated with the spring in its fully wrapped ($\varphi = \varphi_{max}$) position as was shown in the preceding section (2.3.1). This, in turn, may be found on the assumption of an initially flat spring (i.e., prior to assembly in the barrel), without radial pressure. Consider the fully elastic case:

$$M_{\varphi_{max}} = \frac{EI}{\rho}$$

where $M_{\varphi_{max}}$ = maximum spring moment at φ_{max}

ρ = smallest radius of curvature of spring coil = arbor radius when spring is fully wound.

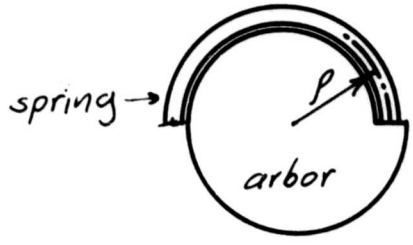

However, it will be found from later numerical considerations that this case does not apply for the fuze springs under consideration. For these springs the plastic case must be considered.

3.2.3.3 Plastic Case

The spring when wound, from an initially flat state, and subjected to an enforced radius of curvature, ρ, however, may be in any one of the following states, with regard to its stress distribution:

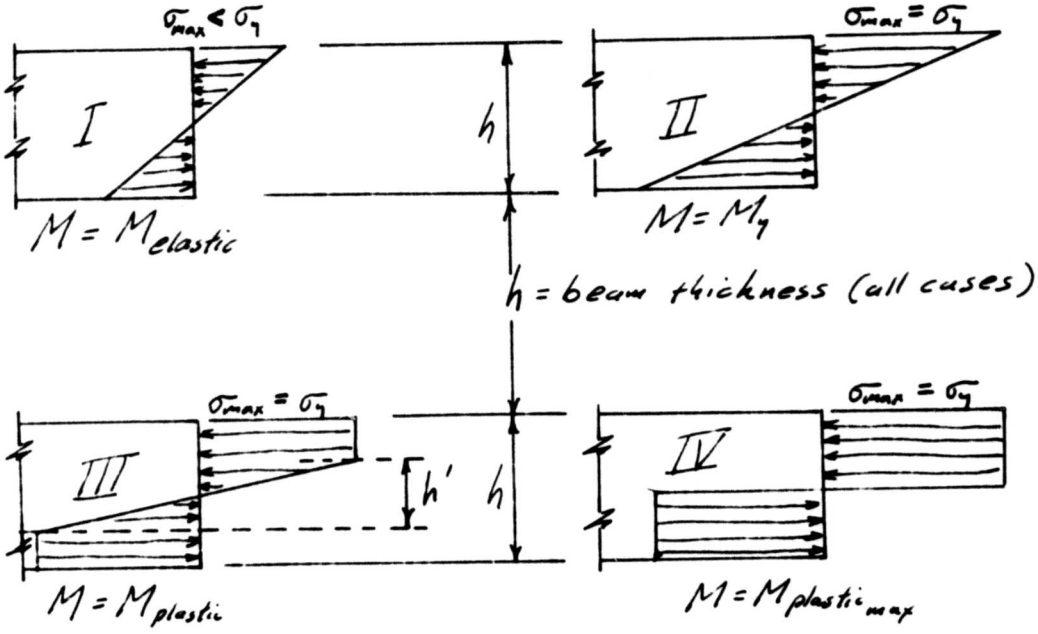

For the range of values encountered in time fuze motor springs, case III must be considered. Note that the maximum bending stress, σ_{max}, is equal to the yield stress, σ_y, in this case, as well as in cases II and IV. In this case, however, there is an elastic core of thickness h'; thus II and IV are special cases of III, with h' equal to zero and to h, respectively.

Thus the moment at the arbor (for case III) can be shown to be given by the relationship

$$M = b\,\sigma_y \left[\left(\frac{h}{2}\right)^2 - \frac{1}{3}\left(\frac{h'}{2}\right)^2 \right]$$

where b = spring width

h = spring thickness

h' = elastic core thickness

The core thickness, h', may be found in terms of the radius of curvature of the spring considering the elastic deformation of the core, i.e.,

$$h' = 2\rho \frac{\sigma_y}{E}$$

Substituting this relationship into the expression for the plastic moment, and noting that $K_1 M_{plastic} = T_{max}$, the maximum spring torque is found to be:

$$T_{max} = K_1 b \sigma_y \left[\left(\frac{h}{2}\right)^2 - \frac{1}{3} \left(\rho \frac{\sigma_y}{E}\right)^2 \right]$$

It may be noted that this expression can be written:

$$T_{max} = K_1 M_{yield} \left[\frac{3}{2} - \frac{1}{2} \left(\frac{\rho \sigma_y}{E \{\frac{h}{2}\}} \right)^2 \right]$$

where $M_{yield} = \sigma_y \left(\frac{bh^2}{6}\right)$, see case II, previous page.

So that the condition $T_{max} = K_1 M_{yield}$ when $\rho = \rho_{min}$ implies that:

$$\left(\frac{\rho \sigma_y}{E \{\frac{h}{2}\}} \right) = 1$$

or:

$$\rho_{min\ elast.} = \frac{E}{\sigma_y} \frac{h}{2}$$

} For initiation of plastic flow

Thus: for $\rho < \rho_{min}$, $T_{max} = K_1 b \sigma_y \left[\left(\frac{h}{2}\right)^2 - \frac{1}{3} \{\rho \frac{\sigma_y}{E}\}^2 \right]$

for $\rho = \rho_{min}$, $T_{max} = K_1 b \sigma_y \frac{h^2}{6}$

for $\rho > \rho_{min}$, $T_{max} = K_1 \frac{EI}{\rho}$

Note that subsequent to the initial deformation of the spring (presumably during the manufacturing process) the spring upon unwinding and rewinding, will return to the T_{max} value in a linear manner (even though T_{max} may exceed $K_1 M$ yield, for $\rho < \rho_{min}$). This statement would be strictly true for an ideal elastic-plastic material, and for a "non-ideal" material is close enough for our present purposes. For an ideal elastic-plastic, the stress-strain curve has the following shape:

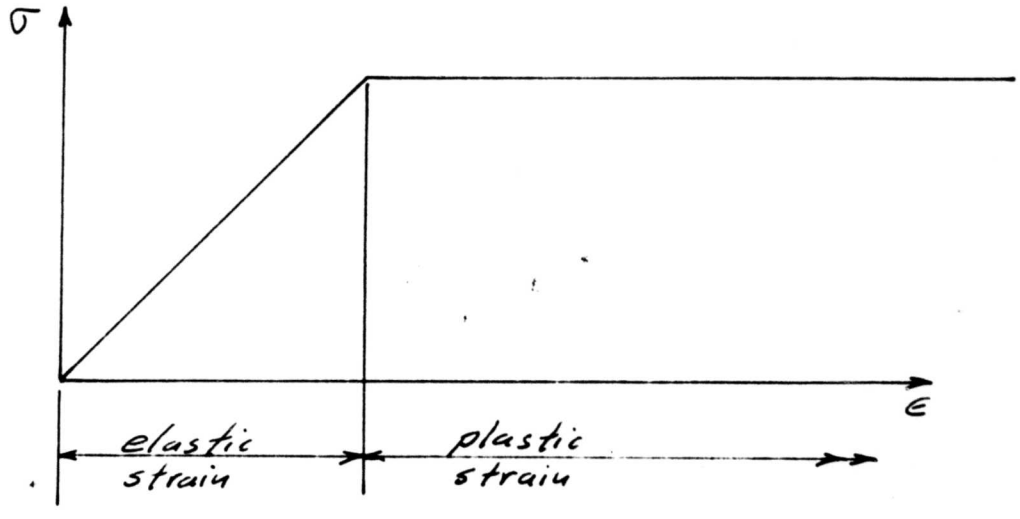

Thus, for multiple deformations the critical elements behave as;

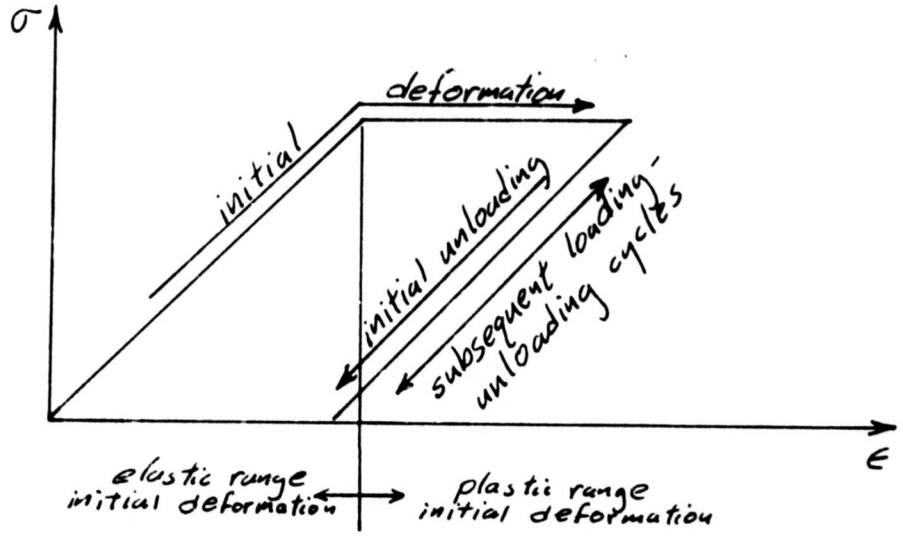

This elastic-plastic loading-unloading cycle on the outer fibers, combined with the elastic loading-unloading cycle on the inner fibers, results in the following stress distributions:

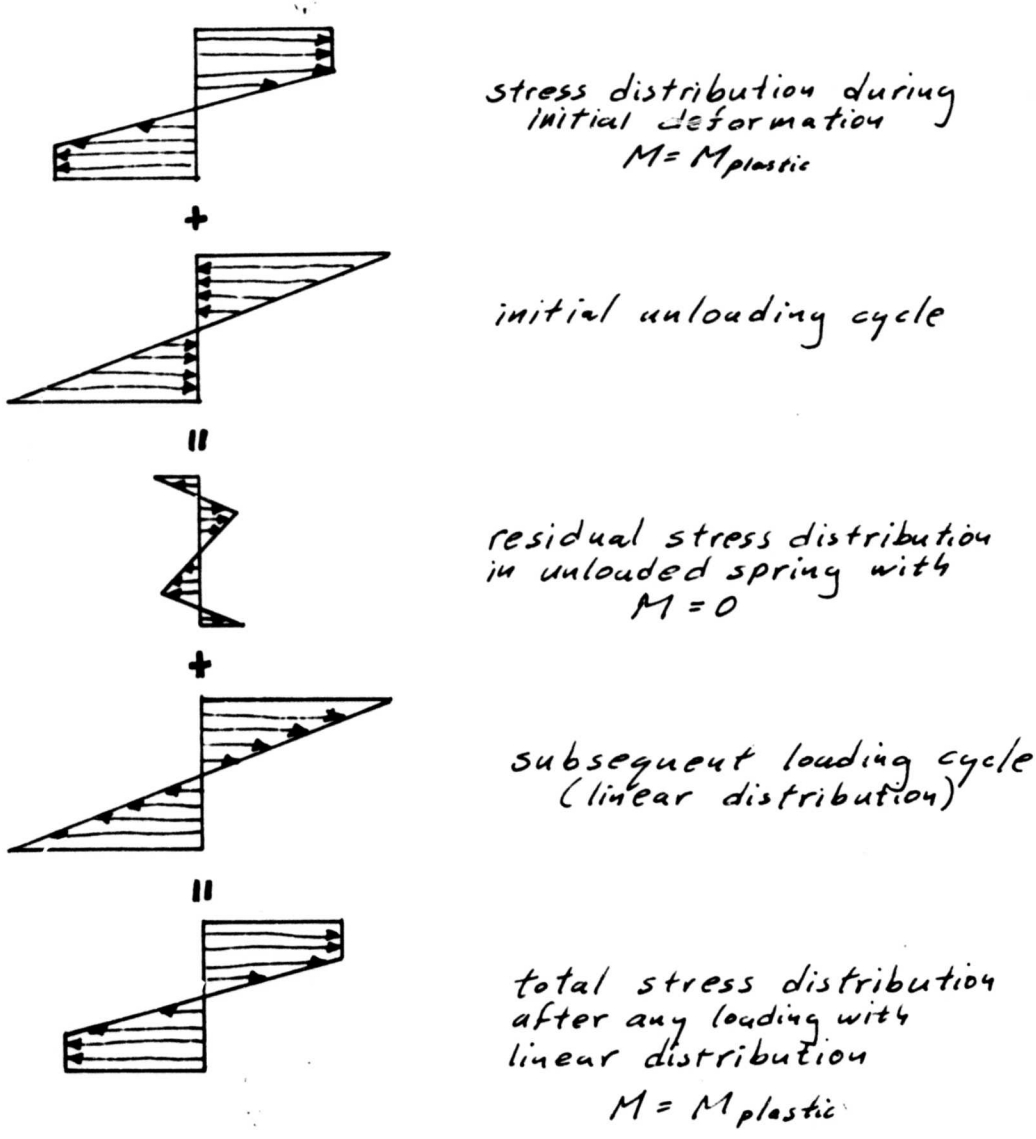

Note that the "apparent" loading and unloading cycle is:

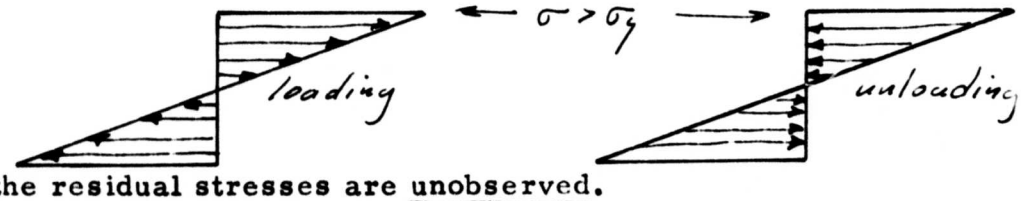

and that the residual stresses are <u>unobserved</u>.

Thus the value of T_{max} is independent of the number of wind-up and unwind cycles imposed on the spring. The torque-turn characteristic ($T-\varphi$) is linear for a range of values of torque up to and including T_{max}. This portion of the curve then is fully determined. The fully unwound portion of the curve falls in a non-linear domain and, being of less interest at the present time, is not treated in this report.

3.3. SPIN EFFECT ON MOTOR SPRING

Let us now consider the effect of spin on the static torque turn characteristic (as discussed in section 3.2). The following assumptions will be utilized in the ensuing study.

(1) The spin environment may be represented by a centrifugal field only, i.e., Coriolis effects are negligible.

(2) The centrifugal field may be represented in a quasi-static manner, i.e., transient effects and other inertial effects are not considered during the initial stages of the investigation.

(3) The bending and "membrane" effects due to the centrifugal field may be treated as uncoupled.

(4) The axisymmetric effects may be treated as uncoupled from any eccentric bending effects.

Assumptions (1), (3) and (4) are made at the outset in order to facilitate the investigations; they may actually be proven valid at a later stage in the investigation, thus becoming conclusions. Assuption (2) merely serves to indicate that the initial investigation seeks a steady-state solution to the problem; transient effects will be considered later, and required modifications may then be applied to the steady-state solution. The steady-state solution yields insight into the mechanism under study and is necessary prior to the more complex transient solution in the course of new analytical investigations; the transient investigation may never be required.

3.3.1 "AXIALLY SYMMETRIC" SOLUTIONS

A spiral is by its geometry, unsymmetrical. For axial symmetry,

$$r(\alpha + \delta\alpha) = r(\alpha)$$

must be everywhere true (i.e., for all α and for all $\delta\alpha$). For a spiral this is not true but it is almost true everywhere. That is:

$$r(\alpha + \delta\alpha) = r(\alpha) + \epsilon$$

where α = any spiral angle

$\delta\alpha$ = change in spiral angle

$\epsilon = \delta\alpha \frac{dr}{d\alpha}$

$\frac{dr}{d\alpha}$ = "pitch of spiral (constant in Archimedean spiral)

For the special case of interest, where $\epsilon \to 0$ (large number of coils), half of any coil is closely approximated by a semi-circle.

The following treatment will initially be limited to those facets of the problem related to the "quasi-symmetrical" spiral.

3.3.1.1 Uncoupled Extensional Deformations

In view of assumption (3), "membrane" and bending effects may be treated separately. Membrane, or extensional deformation, effects will be treated first, where membrane effects are understood to imply effects traceable to net force resultants due to stress distributions across the cross-section of the spring. Bending effects, on the other hand, are understood to imply those effects traceable to stress distributions, having a net moment at the neutral axis of the spring cross-section. Thus any linear stress distribution is merely the superposition of the membrane and the bending stress distributions, as shown below.

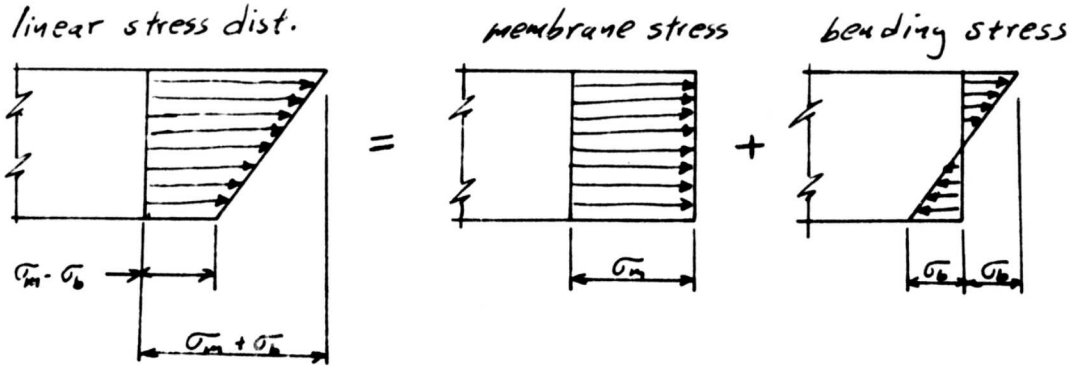

In the following an energy approach will be introduced; which is only one of many techniques which will be utilized.

Based on the "quasi-symmetrical" assumption, one may develop, for the extensional case alone, the following analytical model. Assuming

that each coil may be approximated by a circular arc (i.e., $\frac{4\pi}{\alpha}\delta\alpha \ll r$ for $\delta\alpha < 2\pi$), the following idealization will be utilized:

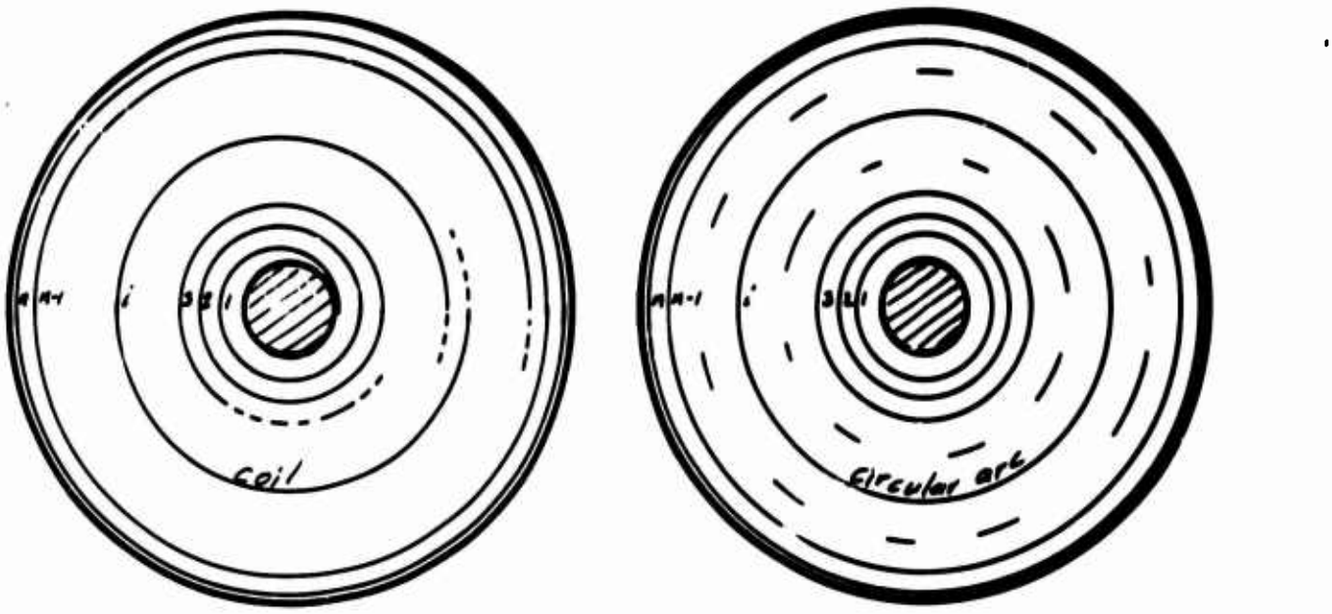

Spring Extensional Idealization (quasi-symmetric)

The element of spring length, for the i^{th} coil, now appears as:

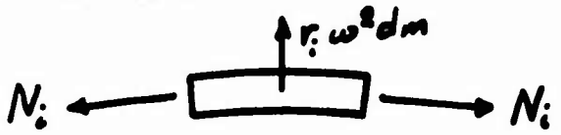

Thus, for equilibrium:

$$N = m\omega^2 r^2 .$$

and the radial growth (u) is given by

$$u = \frac{Nr}{AE} .$$

where the membrane force, N, is constant for any one coil (i.e., for each circular arc).

The theorem on total potential energy of a body (which may be found on page 173 of Love's "Mathematical Theory of Elasticity") states that

$$\Sigma W_{total} = 0$$

where the total potential, ΣW_i, is equal to the sum of the internal (strain) energy, U, of the deformed body, minus one-half the external work done on the body, $\frac{1}{2}W$ (in this case, by the centrifugal forces) in deforming from its unloaded state to its loaded state of equilibrium. Since only "membrane" effects are now being considered the subscript N will be used. Thus:

$$U_N - \tfrac{1}{2} W_N = 0$$

where

$$U_N = \int_l \frac{N^2}{2AE}\, ds$$

$$W_N = \omega^2 \int_l m r^2 u \, d\vartheta \qquad (\Delta r \ll r)$$

N = stress resultant of membrane stresses

AE = spring stiffness in stretching

l = length of spring

s, ϑ = arc length and angle respectively, measured around the spring

r = radius to generic point on spring

m = mass per unit length of spring

ω = spin rate of spring

u = change in r under centrifugal force $(m\omega^2 r \times r\, d\vartheta)$

Integrating W_N for each coil, one finds for the i^{th} coil:

$$W_{N_i} = 2\pi m \omega^2 r_i^2 u_i$$

Thus:

$$W_N = 2\pi m \omega^2 \sum_{i=1}^{n} (r^2 u)_i$$

where the coils are denoted by enumerators, i, $1 \le i \le n$.

Likewise, one finds:

$$U_N = \frac{\pi}{AE} \sum_{i=1}^{n} (N^2 r)_i$$

Substitution in $U_N - \frac{1}{2} W_N = 0$, yields:

$$\sum_{i=1}^{n} (N^2 r)_i - m A E \omega^2 \sum_{i=1}^{n} (r^2 u)_i = 0$$

$$\frac{\sum_{i=1}^{n} (N^2 r)_i}{\sum_{i=1}^{n} (r^2 u)_i} = m A E \omega^2$$

Substituting the i^{th} coil displacement relation:

$$u = \frac{Nr}{AE}$$

the general expression for all coils may be written:

$$\frac{\sum_{i=1}^{n} (N^2 r)_i}{\sum_{i=1}^{n} (r^3 N)_i} = m \omega^2$$

The above expression holds in general and, as can be shown, for the i^{th} and j^{th} coils;

$$\frac{N_i^2 r_i}{r_i^3 N_i} = \frac{N_j^2 r_j}{r_j^3 N_j} = m \omega^2$$

or

$$\frac{N}{r^2} = \text{constant} = m \omega^2$$

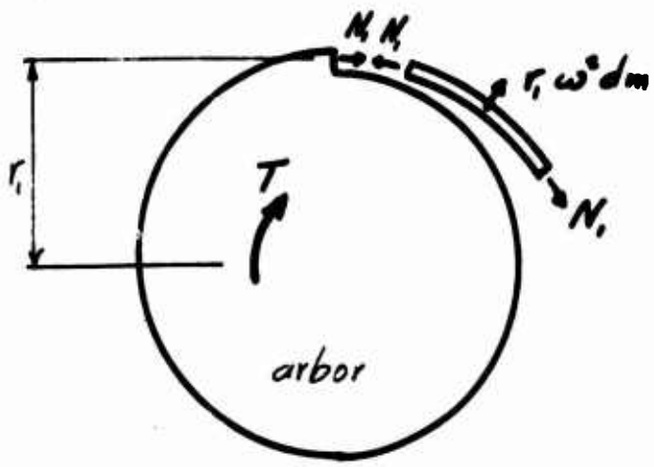

This is the result that is obtained by an equilibrium analysis of a hoop (or a thin cylindrical shell) of radius r and body force equal to the value $m\omega^2 r$. The mechanism involved in the stretching of the spring is akin to that involved in the stretching of the hoop; an order-of-magnitude estimate of the value of $N = N_1$ (i.e., the uncoupled membrane force, alone) at the juncture of spring and arbor can be arrived at by

$$N_1 = m\omega^2 r_1^2$$

where:

N_1 = spring membrane force at arbor

r_1 = arbor radius

$m = \rho A$ (mass per unit length)

The additional torque due to a spring membrane force of this magnitude at the arbor is simply

$$T_N = N_1 r_1 = m\omega^2 r_1^3$$

For constant ω, the value of T_N is approximately constant throughout the unwinding cycle, except when the unwinding angle, φ, is close to the limits, zero and φ_{max}. At these points, and close to them, various parameters are affected by the fact that coils are effectively taken out of operation by being pressed against either the arbor or the barrel.

The membrane effect on the value of T_N found for the particular case of the spring configuration being investigated

$r_1 = .1"$ $\quad \omega = 3140$ rad/sec

$b = .15"$ $\quad m = \frac{.3}{386} \times bh$ #-sec^2-in

$h = .01"$

is approximately $\frac{1}{4}$ in-oz, which is about 1.2% of the maximum static torque of 20.5 in-oz. A percentage deviation of this magnitude may not be considered important. It is to be emphasized, however, that this represents only one portion of the total dynamic effect, so it will not be investigated in further detail until all the effects are examined; and is subject to further experimental verification.

3.3.1.2 Bending Deformations

3.3.1.2.1 Axi-Symmetric Deformations

Axi-symmetrical" bending deformations represent a redistribution of coils within the radial confines of the barrel and arbor, as the spring is spun up. In addition to these boundary constraints, spring bending deformations must satisfy constant spring length and invarient total number of coils (since the spring is taken in a position of quasi-steady wind position) conditions. These reflect the conditions which must be imposed on the deformation since membrane extension was found to be small.

All deformations which represent geometrically possible coil distributions can be classified in the following manner:

Class (1): Uniform distribution which will be assumed to correspond to the initial undeformed state of the spring.

(Let n_1, n_2, and n_3 represent arbitrary numbers such that $n_1 + n_2 + n_3 = n =$ total number of coils of spring, $n_i \geq 0$)

Then class (2) and (3) deformations may be defined as:

Class (2):
- n_1 outer coils move outward (toward barrel)
- n_2 inner coils move inward (toward arbor)
- n_3 coils remain stationary (in class (1) distribution)

Class (3):
- n_1 outer coils move inward (toward median radius)
- n_2 inner coils move outward (toward median radius)
- n_3 coils remain stationary (in class (1) distribution)

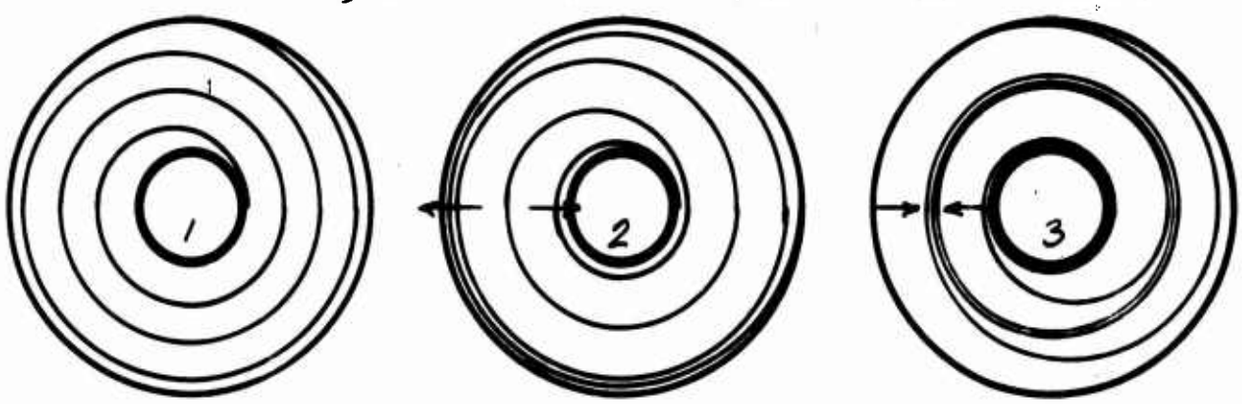

For further consideration each coil will be taken to have a constant radius (r_i) with an intercoil spacing (Δr_i); which greatly simplifies the ensuing analysis while retaining the important basic physical parameters. Thus the above figures are idealized as

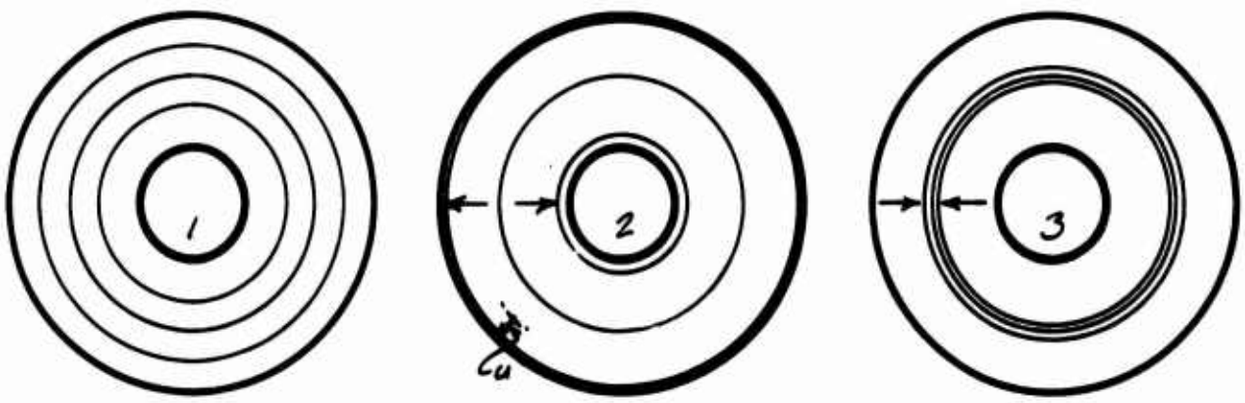

u_i = radial deflection of "i" coil, (positive sign taken outward)

It is understood that in this schematic representation the coils are considered "open" so that no membrane stress exists and that each coil occupies a full 360° (except possibly the first and last) transporting whatever material is required from its neighboring coil.

The foregoing classification as to types of deformation, facilitates the utilization of the theorem of minimum potential energy. As stated in section 15 (Mechanics of Materials) of the McGraw-Hill Mechanical Design and Systems Handbook, the theorem is: "Among all states of strain which satisfy the strain-displacement relationships and displacement boundary conditions the associated stress state, derivable through the stress-strain relationships, which also satisfies the equilibrium equations, is determined by the "minimization" of Π where

$$\Pi = \int_{vol.} \bar{U} dV - \int_{surface} (\bar{p}_x u + \bar{p}_y v + \bar{p}_z w) dS$$

where $\bar{p}_x, \bar{p}_y, \bar{p}_z$ are the x, y, z components of any prescribed surface stresses."

The function Π may be expressed, in the notation of this report:

$$\Pi = U - W$$

where U = total strain energy of deformation from equilibrium position to any particular deformed position, and W = work done by centrifugal forces during the same deformation.

The following highly simplified example is illustrative of the manner in which the above theorem will be utilized in this report.

Example:

Let us find the deformation of a simple extension spring (spring constant = k), under the influence of a force F , with preload F_o .

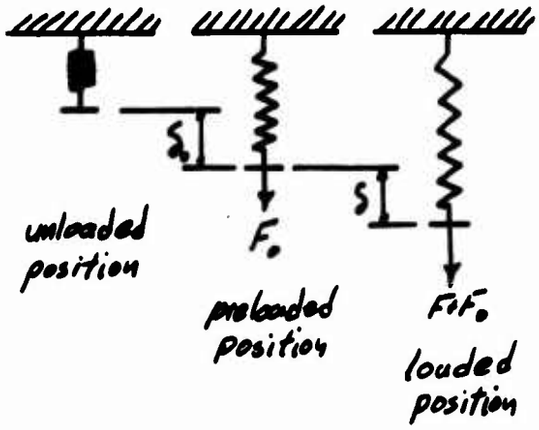

Let us consider δ_o the equilibrated deformation which, in this case, satisfies the equation

$$F_o - \delta_o k = 0$$

The theorem of minimum potential can be applied to either the original or the preloaded system to provide the same result; except that in the former the preloaded equilibrium equation must be known and utilized.

(1) Total System $(\delta > 0)$

$$W = F_o(\delta + \delta_o) + F\delta$$

$$U = \tfrac{1}{2} k (\delta + \delta_o)^2$$

hence

$$\Pi = \tfrac{1}{2} k (\delta + \delta_o)^2 - [F\delta + F_o(\delta + \delta_o)]$$

$$\Pi = \frac{k\delta}{2}\left[\delta - \frac{2F}{k}\right] + \delta[k\delta_o - F_o] + \frac{k\delta_o}{2}\left[\delta_o - \frac{2F_o}{k}\right]$$

$k\delta_o - F_o = 0$ (from equilibrium equation)

It is now necessary to minimize Π with respect to all possible variations in δ . This could be done by setting $\frac{\partial \Pi}{\partial \delta} = 0$. However, since this

technique may not be applicable in this report, we will consider the most general illustrative technique of actually presenting the result graphically. For this purpose we plot Π vs. δ for $\delta \geq 0$.

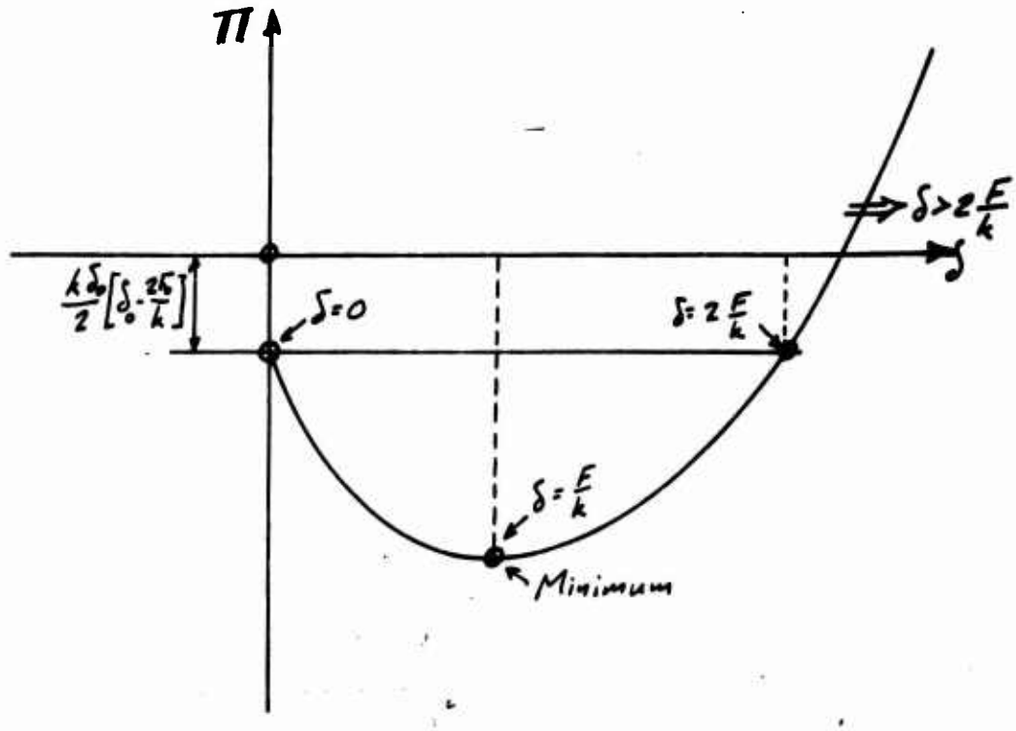

We see that the minimum Π occurs at

$$\delta = \frac{F}{k}$$

which represents the desired solution.

(2) Relative System ($\delta > 0$)

In this case we consider only the perturbation from the equilibrium system so that it is not necessary to utilize the preload equilibrium equations (no matter what their complexity). Thus

$$W = F\delta$$

$$U = \frac{1}{2} k \delta^2$$

hence

$$\Pi = \tfrac{1}{2} k \delta^2 - F\delta$$

or

$$\Pi = \frac{k\delta}{2}\left[\delta - 2\frac{F}{k}\right]$$

which plots similarly as

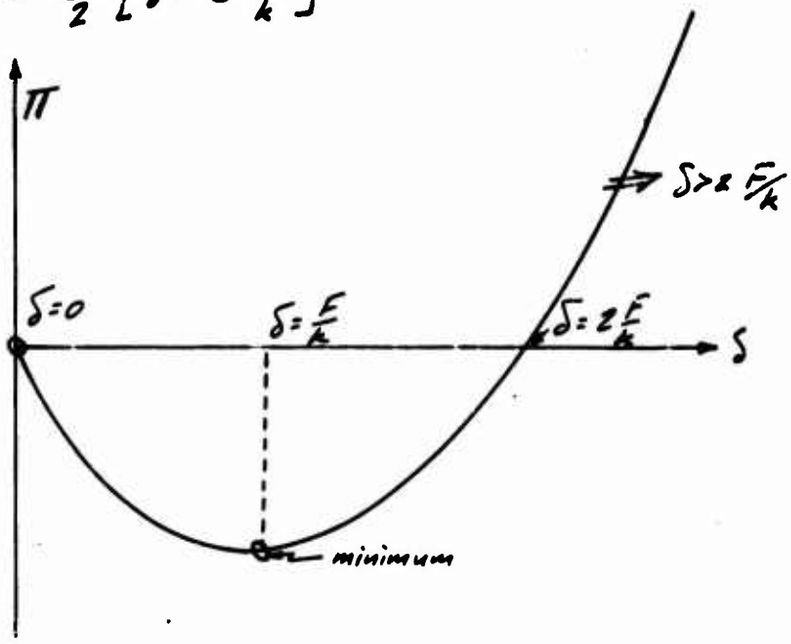

and yields a minimum where $\delta = \frac{F}{k}$, which is the desired solution.

For the purposes of the work of this report we will always consider the spin perturbations from the non-spin equilibrium position; which greatly improves and simplifies the minimization procedure.

3.3.1.2.2 Elimination of Class (3) Deformation

In order for the assumed deformation pattern from class (1) to any other class, to be possible, the function Π must decrease. Thus:

$\Pi_{(2)} < 0$ is required

Since $\Pi_{(1)} = 0$ is the reference position.

However, $$\Pi = U_{(n)} - W_{(1\to n)}$$

thus, the possibility requirement becomes

$$U_{(n)} < W_{(1\to n)}$$

but, $U_{(n)} > 0$ for all deformations

therefore it is <u>necessary</u> (but not sufficient) that

$$W_{(1\to n)} > 0$$

in order to satisfy the requirement.

The work for the i^{th} coil, in moving from the non-spin position to the perturbed position, is given by

$$W_i = \int_0^{2\pi} \overbrace{(m r_i d\vartheta)}^{dm} \omega^2 r_i u_i$$

and the total work of all the coils due to the perturbation is,

$$W = 2\pi m \omega^2 \sum_{i=1}^{n} r_i^2 u_i$$

where

r_i = average i^{th} coil radius

u_i = change in i^{th} coil radius.

Now considering the class (3) deformation

$$u_i < 0 \ , \ n_1 \text{ coils} \ , \ r_i \geq r'_{(3)}$$
$$u_i = 0 \ , \ n_3 \text{ coils} \ , \ r''_{(3)} \leq r_i \leq r'_{(3)}$$
$$u_i > 0 \ , \ n_2 \text{ coils} \ , \ r_i \leq r''_{(3)}$$

and using the absolute magnitudes of deformations, we can rewrite the work as

$$W = 2\pi m \omega^2 \left[-\sum_{i=1}^{n_1} r_i^2 |u_i| + \sum_{i=1}^{n_2} r_i^2 |u_i| \right]$$

Considering the upper bound

$$W \leq 2\pi m \omega^2 \left[-r'^2_{(s)} \sum_{i=1}^{n_1} |u_i| + r''^2_{(s)} \sum_{i=1}^{n_2} |u_i| \right]$$

However, considering the total coil length

$$L_o = 2\pi \sum_{i=1}^{n} r_i \qquad \text{(non-spinning)}$$

$$L_f = 2\pi \sum_{i=1}^{n} (r_i + u_i) \qquad \text{(spinning)}$$

But from the requirement for constant length

$$L_o = L_f$$

or

$$\sum_{i=1}^{n} r_i = \sum_{i=1}^{n} (r_i + u_i)$$

which requires

$$\sum_{i=1}^{n} u_i = 0$$

or

$$\sum_{i=1}^{(n_1)} |u_i| = \sum_{i=1}^{(n_2)} |u_i|$$

thus

$$W \leq 2\pi m \omega^2 \sum_{i=1}^{n_1} |u_i| \left[r''^2_{(s)} - r'^2_{(s)} \right]$$

since $r_3'' \leq r_3'$

$\therefore \quad W \leq 0$

which is a direct violation of our requirement, so that **class (3) deformations cannot exist.**

3.3.1.2.3 Axially-Symmetric Bending Deformation Pattern

In accordance with the idealization set forth in preceding sections, the spring system, with its governing equations is presented below for reference:

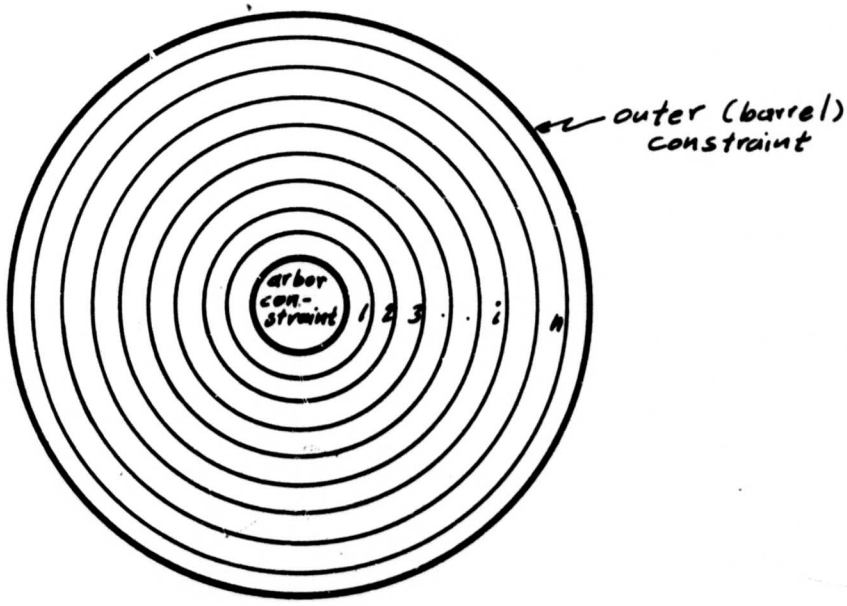

$\Pi = U - W$ ⇒ Potential function

$W = 2\pi\omega^2 m \sum_{i=1}^{n} r_i^2 u_i$

$U = \pi EI \sum_{i=1}^{n} \frac{u_i^2}{r_i^3}$

} ⇒ Energy Expressions (See Appendix for discussion)

$\sum_{i=1}^{n} u_i = 0$ ⇒ "Constant Length Condition" insures that length of deformed spring = that of undeformed spring.

It is required that Π be a minimum, within the bounds of the constraints of the problem. This requirement may be formulated as:

$$\underset{(\text{all } i)}{\frac{\partial \Pi}{\partial u_i}} = 0 = \underset{(i \neq n)}{\frac{\partial \Pi}{\partial u_i}} + \frac{\partial \Pi}{\partial u_n} \frac{\partial u_n}{\partial u_i}$$

which together with the constant length condition, as written below, defines a linear set of equations:

$$u_n + \sum_{i=1}^{n-1} u_i = 0$$

From the above form of the constant length condition, one finds that for any $i \neq n$:

$$\frac{\partial u_n}{\partial u_i} = -1$$

and from the energy expressions:

$(i \neq n)$ $\quad \frac{\partial W}{\partial u_i} = 2\pi \omega^2 m r_i^2$

$$\frac{\partial W}{\partial u_n} = 2\pi \omega^2 m r_n^2$$

$(i \neq n)$ $\quad \frac{\partial U}{\partial u_i} = 2\pi EI \frac{u_i}{r_i^3}$

$$\frac{\partial U}{\partial u_n} = 2\pi EI \frac{u_n}{r_n^3}$$

Thus, the equations may be expressed:

$$\begin{cases} u_i - R_i^3 u_n = K R_i^3 (R_i^2 - 1) & , (i \neq n) \\ \sum_{i=1}^{n} u_i = 0 \end{cases}$$

where, $K = \frac{\omega^2 m r_n^5}{EI}$

$R_i = \frac{r_i}{r_n}$

$m = \rho A$ (mass density × cross-sectional area)

Solving for u_i $(i \neq n)$ one finds:

$$u_i = K R_i^3 (R_i^2 - 1) + R_i^3 u_n$$

Substitution of the above value of u_i in the constant length condition equation $\sum_i^n u_i = 0$, yields:

$$u_n + \sum_{i=1}^{n-1} R_i^3 K (R_i^2 - 1) + \sum_{i=1}^{n-1} R_i^3 u_n = 0$$

Therefore

$$u_n = -K \left[\frac{\sum_{i=1}^{n-1} R_i^3 (R_i^2 - 1)}{1 + \sum_{i=1}^{n-1} R_i^3} \right]$$

so that all u_i can now be calculated. It will prove convenient to take r_n (at the arbor) since it is often sufficient to compute this value alone in the evaluation of spring torque. A sample calculation is presented in the Appendix B.

In the event that coils bottom out against each other or the barrel, or if $u_i \not< r_i$ then it is necessary to proceed with the "new configuration" step by step in an iterative procedure. To examine this iterative process let us proceed as follows:

The following definitions apply to this analysis.

Let

n = total number of coils during j^{th} iteration

j = iteration index (j^{th} iteration $\Rightarrow$ present iteration)

i = coil index ($1 \leq i \leq n$)

Then the "non-equilibrated" incremental force (acting on the i^{th} coil, during the j^{th} iteration) is given by

$$\Delta F = (dm \omega^2 r_i)^{(j)} - (dm \omega^2 r_i)^{(j-1)}$$

and the additional i^{th} coil displacement during the j^{th} iteration (not the total i^{th} coil displacement) is $(u_i)^{(j)}$. Thus the j^{th} iteration work done in coil displacement is

$$W^{(j)} = \sum_{i=1}^{n} (W_i)^{(j)} = \sum_{i=1}^{n} \left(u_i \int_0^{2\pi} \Delta F_i \right)^{(j)}$$

Expressing the differential mass in terms of a differential coil length (of the form $r d\varphi$), for the j^{th} and preceding iteration:

$$dm^{(j)} = m (r_i)^{(j)} d\varphi \; ; \quad dm^{(j-1)} = m (r_i)^{(j-1)} d\varphi$$

Thus the expression for work becomes

$$W^{(j)} = 2\pi m \sum_{i=1}^{n} \left[\omega^{(j)^2} (r_i)^{(j)^2} - \omega^{(j-1)^2} (r_i)^{(j-1)^2} \right] (u_i)^{(j)}$$

or

$$W^{(j)} = 2\pi m \, \omega^{(j)^2} \sum_{i=1}^{n} (S_i)^{(j)} (r_i u_i)^{(j)}$$

where

$$(S_i)^{(j)} = \left[1 - \left(\frac{\omega^{(j-1)}}{\omega^{(j)}} \right)^2 \left(\frac{r_i^{(j-1)}}{r_i^{(j)}} \right)^2 \right]$$

In order to minimise the potential, Π, for the j^{th} iteration, analogous to the non-iterative procedure (which corresponds to the $j = 1$ iteration), the strain energy, $U^{(j)}$, expression is likewise required. $U^{(j)}$ represents the incremental strain energy associated with the change from the $(j-1)$ to the (j) position of all coils, i.e.,

$$U^{(j)} = \pi E I \sum_{i=1}^{n} \left(\frac{u_i^2}{r_i^3} \right)^{(j)}$$

Likewise, the constant length condition must be employed for each iteration. For the j^{th} iteration, it is required that

$$\sum_{i=1}^{n} (u_i)^{(j)} = 0$$

where it is to be noted that $(u_i)^{(j)}$ represents the additional displacement which occurs during the j^{th} iteration.

Thus the governing equations have been found to be expressible in the following form

$$\Pi^{(j)} = U^{(j)} - W^{(j)} \Rightarrow \text{Potential Function}$$

$$\left.\begin{aligned} W^{(j)} &= 2\pi m \omega^{(j)^2} \sum_{i=1}^{n} (s_i)^{(j)} (r_i^2 u_i)^{(j)} \\ U^{(j)} &= \pi E I \sum_{i=1}^{n} \left(\frac{u_i^2}{r_i^3}\right)^{(j)} \end{aligned}\right\} \text{Energy Expressions}$$

$$\sum_{i=1}^{n} (u_i)^{(j)} = 0 \Rightarrow \text{"Constant Length" Condition}$$

Note that for the case $j=1$, the above equations reduce to those presented for the non-iterative case, since $\delta_i^{(1)} = 1$.

It is required that $\Pi^{(j)}$ be a minimum, within the bounds of the constraints of the problem. This requirement may be formulated as:

$$\frac{\partial \Pi^{(j)}}{\partial (u_i)^{(j)}} = 0 = \frac{\partial \Pi^{(j)}}{\partial (u_i)^{(j)}} + \frac{\partial \Pi^{(j)}}{\partial (u_n)^{(j)}} \frac{\partial (u_n)^{(j)}}{\partial (u_i)^{(j)}}$$

which, together with the constant length condition, as written below, defines a linear set of equations:

$$(u_n)^{(j)} + \sum_{i=1}^{n-1} (u_i)^{(j)} = 0$$

From the above form of the constant length condition, one finds that for any $i \neq n$:

$$\frac{\partial (u_n)^{(j)}}{\partial (u_i)^{(j)}} = -1$$

and from the energy expressions:

$$(i \neq n) \quad \frac{\partial W^{(j)}}{\partial (u_i)^{(j)}} = 2\pi m \omega^{(j)^2} S_i^{(j)} r_i^{(j)^2}$$

$$\frac{\partial W^{(j)}}{\partial (u_n)^{(j)}} = 2\pi m \omega^{(j)^2} S_n^{(j)} r_n^{(j)^2}$$

$$(i \neq n) \quad \frac{\partial U^{(j)}}{\partial (u_i)^{(j)}} = 2\pi E I \frac{u_i^{(j)}}{r_i^{(j)^3}}$$

$$\frac{\partial U^{(j)}}{\partial (u_n)^{(j)}} = 2\pi E I \frac{u_n^{(j)}}{r_i^{(j)^3}}$$

Thus the equations may be expressed:

$$\begin{cases} u_i^{(j)} - R_i^{(j)^3} u_n^{(j)} = K^{(j)} R_i^{(j)^3} \left[\alpha_i^{(j)} R_i^{(j)^2} - 1 \right] \\ \sum_{i=1}^{n} (u_i)^{(j)} = 0 \end{cases}$$

where

$$R_i^{(j)} = \frac{r_i^{(j)}}{r_n^{(j)}}$$

$$\alpha_i^{(j)} = \frac{S_i^{(j)}}{S_n^{(j)}}$$

$$K^{(j)} = \frac{m \omega^{(j)^2}}{EI} r_n^{(j)^5} S_n^{(j)}$$

Solving for $(u_i)^{(j)}$, $(i \neq n)$ and for $(u_n)^{(j)}$, one finds:

$$(u_i)^{(j)} = K^{(j)} R_i^{(j)3} \left[\alpha_i^{(j)} R_i^{(j)2} - 1 \right] + R_i^{(j)3} u_n^{(j)}$$

$$(u_n)^{(j)} = -K^{(j)} \left[\frac{\sum_{i=1}^{n-1} R_i^{(j)3} \left\{ \alpha_i^{(j)} R_i^{(j)2} - 1 \right\}}{1 + \sum_{i=1}^{n-1} R_i^{(j)3}} \right]$$

Again it is found that for the case $j=1$, the above expressions reduce to those of the non-iterative case, i.e.,

for $j=1$ $\quad S_i^{(1)} = 1$

and $\quad S_n^{(1)} = 1$

thus $\quad \alpha_i^{(1)} = \frac{S_i^{(1)}}{S_n^{(1)}} = 1$

Therefore

$$u_i^{(1)} = K R_i^3 \left[R_i - 1 \right] + R_i^3 u_n$$

$$u_n^{(1)} = -K \left[\frac{\sum_{i=1}^{n-1} R_i^3 \left\{ R_i^2 - 1 \right\}}{1 + \sum_{i=1}^{n-1} R_i^3} \right]$$

which, as was expected, are the non-iterative expressions, u_i and u_n, respectively.

Note that, in general, the summation is over the $n-1$ coils which are <u>not</u> touching. The number of coils which are touching is variable over the iterations, i.e., $n,(j=1) \neq n,(j)$. Thus a symbol of the form $n^{(j)}$ would be justified for use as the summation limit, but would add additional complexity to the notation without being necessary.

The iterative expressions for the displacements, u, are not simple functions of ω^2 or of $\omega^{(j)2}$ since S and A contain $\omega^{(j-1)2}$. Therefore, to solve, a true iterative procedure must be utilized, so that $\omega^{(j-1)}$ is always known from the preceding iteration. Then selecting the new $\omega = \omega^{(j)}$, the constants may be calculated and the displacements obtained.

This is shown schematically below for two coils, the i^{th} and x^{th} with radial position, r, plotted against spin rate ω. Note that the displacement, which is added to those preceding it, is associated with the j^{th} iteration. The j^{th} iteration, in turn, extends the range of the solution from the preceding limit $\omega^{(j-1)}$ to $\omega^{(j)}$ by starting from the base $r_i^{(j)} = r_i^{(j-1)} + u_i^{(j-1)}$.

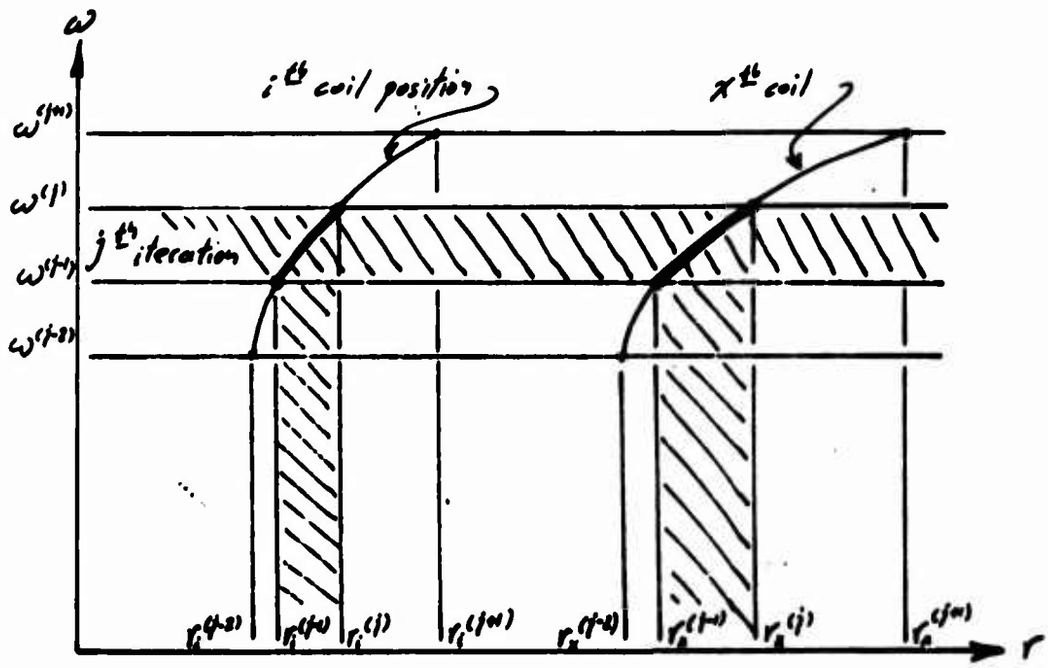

In the same manner, the following iteration will extend the solution to $\omega^{(j+1)}$ from $\omega^{(j)}$ by starting from the base $r_i^{(j+1)} = r_i^{(j)} + u_i^{(j)}$ and calculating $u_i^{(j+1)}$. The only limitation upon this procedure is that each iterative step be sufficiently small so that the ratio

$$\frac{r_i^{(j-1)}}{r_i^{(j)}} \approx 1.$$

In certain special cases where $u_i^{(j)} \ll r^{(j-1)}$ we find that

$$S_i^{(j)} \approx \left[1 - \left(\frac{\omega^{(j-1)}}{\omega^{(j)}}\right)^2\right]$$

Therefore

$$A_i^{(j)} \approx 1$$

Thus the iterative procedure may be pursued for any number of cycles, j, without limiting the break-off point to that at which the effective outer coil is removed from the system. The range of each cycle can be made as small as one pleases, thus yielding a mechanism for insuring the condition $u_i^{(j)} \ll r_i^{(j)}$ for each cycle of calculation. This special case was utilized in the special example computed in section 2.1.2.3.1; but its validity would have to be verified in each application, so that it is better to use the more general relationship for $A_i^{(j)}$.

3.3.1.2.3.1 Example (Spin-induced bending deformation)

Interpretation of the foregoing expression for the deformation, u, will be facilitated by considering a numerical example. For this purpose the following set of physical characteristics will be assumed:

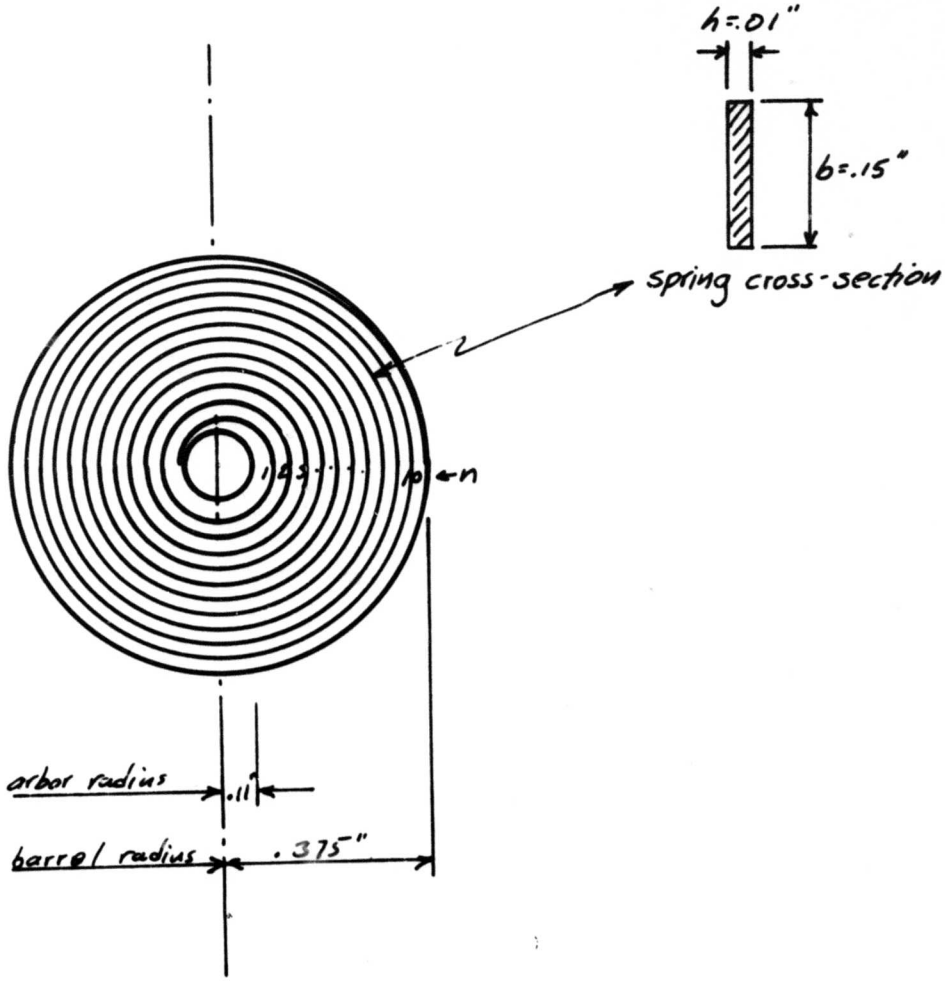

It will be assumed that the idealized spring for this example (i.e., the spring with circular coils) may be represented by the coil radius distribution

$$r = .1 + .025\, i \quad , \quad 1 \le i \le 10$$

Thus the length of spring, l, is found to be $l = .475\,\pi \left(= 2\pi \sum_{i=1}^{10} r_i \right)$

and the inner coil ($r_1 = .125"$) is separated from the arbor by a clearance of

(.125 - .11)= .015". Note that it is assumed here that the position of the spring coil is determined only by the position of its centerline, and that the physical thickness of the spring does not cause interference.

With this inner coil clearance, it is implicit that the inner coil motion, Δr, from the fully wound position of the spring is likewise,

$$\Delta r = .015"$$

Thus, for the non-spinning spring, the torque decrease from the fully wound position is given by (fixed, end case):

$$\Delta T = EI \frac{\Delta r}{r^2}$$

Using the numerical values

$$E = 30 \times 10^6 \text{ psi.}$$
$$I = \frac{1}{12} bh^3 = .0125 \times 10^{-6} \text{ in.}^4$$
$$r = .11 \text{ in.}$$

one finds

$$\Delta T = 7.44 \text{ in.-oz.}$$

Thus, this hypothetical spring has unwound to the point where its non-spinning torque is decreased by the amount 7.44 in-oz. This corresponds to an unwinding angle ($\varphi_{max} - \varphi$) as indicated in the linear elastic spring run down equation,

$$(\varphi_{max} - \varphi) = \frac{l}{EI} (T_{max} - T)$$
$$(\varphi_{max} - \varphi) = 7.85\pi \qquad (\Rightarrow 3.98 \text{ turns})$$

For this same spring, the maximum torque (at the fully wound position) is given by

$$T_{max} = b \sigma_y \left[\left(\frac{h}{2}\right)^2 - \frac{1}{2} \left(\rho \frac{\sigma_y}{E}\right)^2 \right]$$

Thus for a spring material for which the yield stress, $\sigma_y = 300{,}000$ psi, the maximum (fully wound) torque is given by

$$T_{max} = 17.71 \text{ in-oz.}$$

Thus the following non-spinning characteristic may be drawn for the spiral spring of this example.

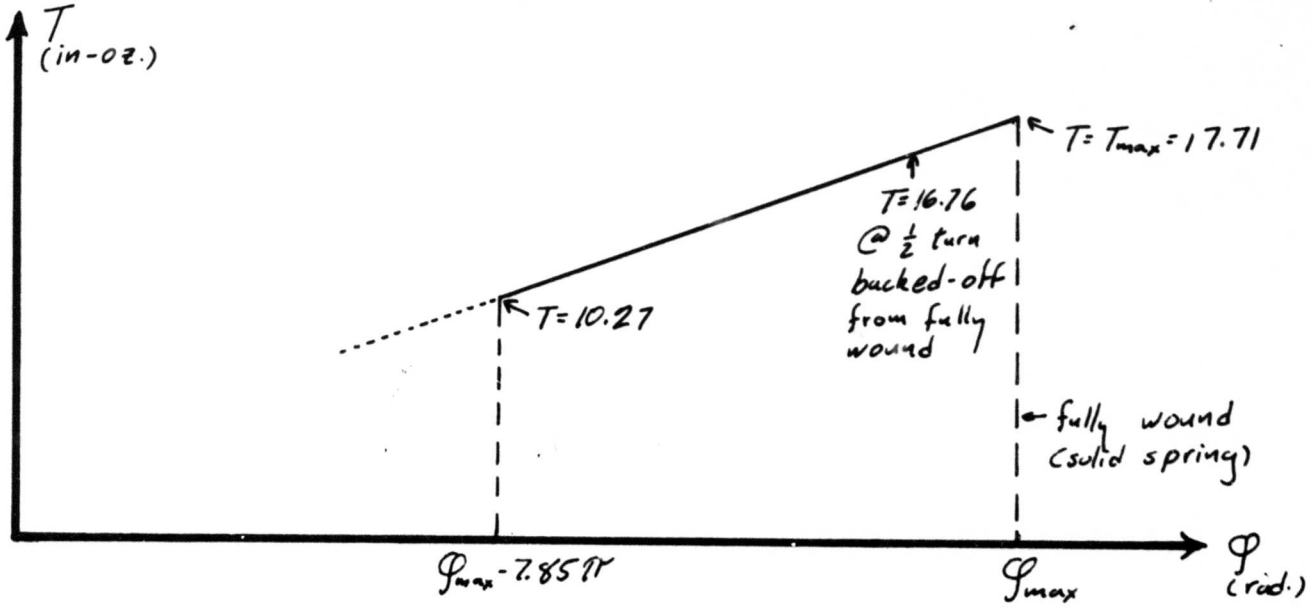

The remainder of the example will be concerned with the determination of the effect upon the spring, of spin induced bending deformation; where the initial condition of the spring is determined by the point on the non-spinning run down characteristic:

$$T = 10.27 \text{ in.-oz.}, \quad \varphi_{max} - \varphi = 7.85\pi .$$

Spring Idealization

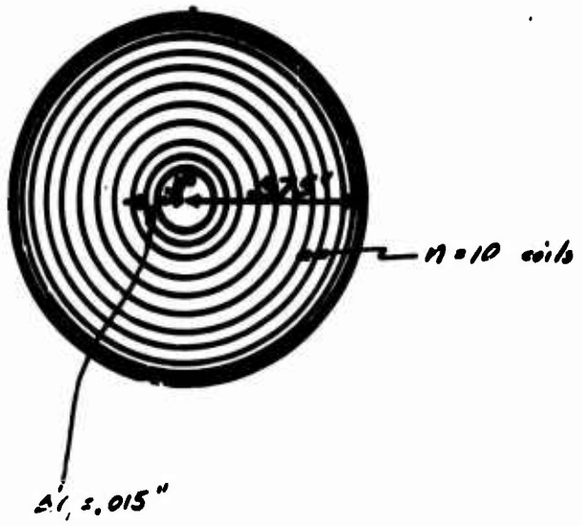

The profile of coil deformation under these conditions is sh.. on the following page, as a function of K. Note that a form of iterative procedure must be used here since at $K \approx$ 20(inches) , coil #10 contacts the outer constraint. For this reason, a second cycle of numerical calculations is initiated at this level of K with a nine coil spring and initial radii $(r_i)_2$ which correspond to the final deformed radii of the first cycle calculation $(r_i + u_i|_{k=20})_1$.

This process is continued on the curve, with succeeding coils being effectively removed from the system by conforming to the shape of

36

Deformation of 10 Coil Spiral Spring in Ce

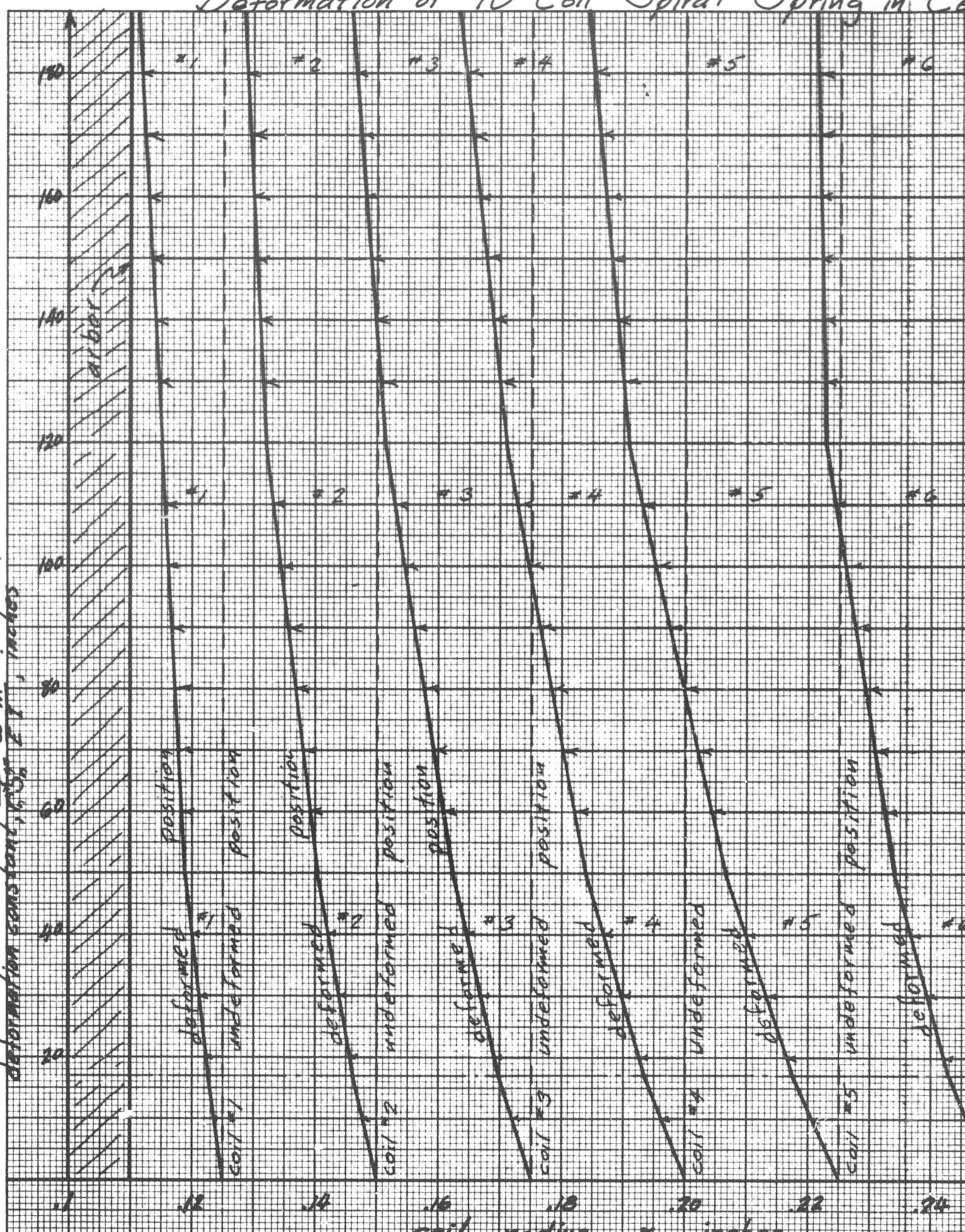

ring in Centrifugal Field (with $r_i = .1"$, $r_o = .375"$)

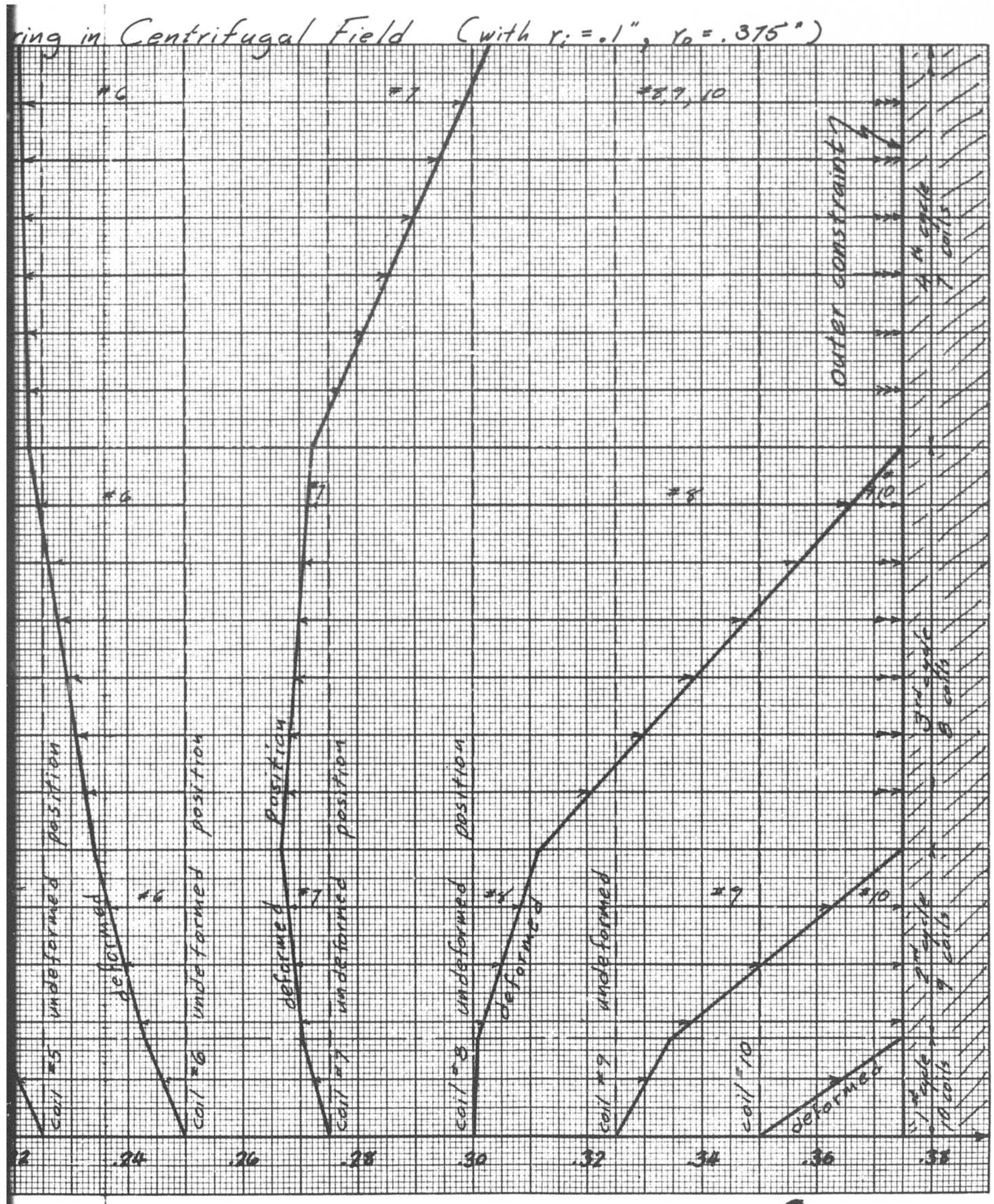

the outer casing, with increasing K. For a given spring configuration, increasing K implies increasing spin velocity, ω, since $K = \frac{\omega^2 m r_o^5}{EI}$ Thus although the deformation expressions utilized in this section are linear with K, they are functions of the square of rotational velocity.

Notice that the maximum values of u_i in the preceding example are:

Cycle	u_i (max)	Corresponding r_i	% of r_i which = u_i
1	.025	.350	7.1%
2	.041	.334	12.2%
3	.063	.311	20.2%

This indicates that it may be desirable to make the later cycles smaller in order to keep u_i about 10% of r_i; or to utilize the full solution for α_i.

The motion of the inner coil is of the greatest interest, since the position of this coil indicates the bending torque being supplied to the arbor. The change in this torque is indicated in the following section.

3.3.1.2.3.2 Torque Sensitivity to Spin in Example

The important torque values to consider in interpreting the spin sensitivity of the spring, are shown on the following curves. The torque associated with the spinning spring is found from the geometry of its inner coil (see preceding curve sheet, coil #1). Since for the present case T is initially equal to 10.27 in.-oz.,

$$\Delta T = 10.27 - \frac{\Delta r}{r^2} EI$$

Thus (for this hypothetical example only) the maximum torque increase due to spin induced, axisymmetric bending is 8% of the static value.

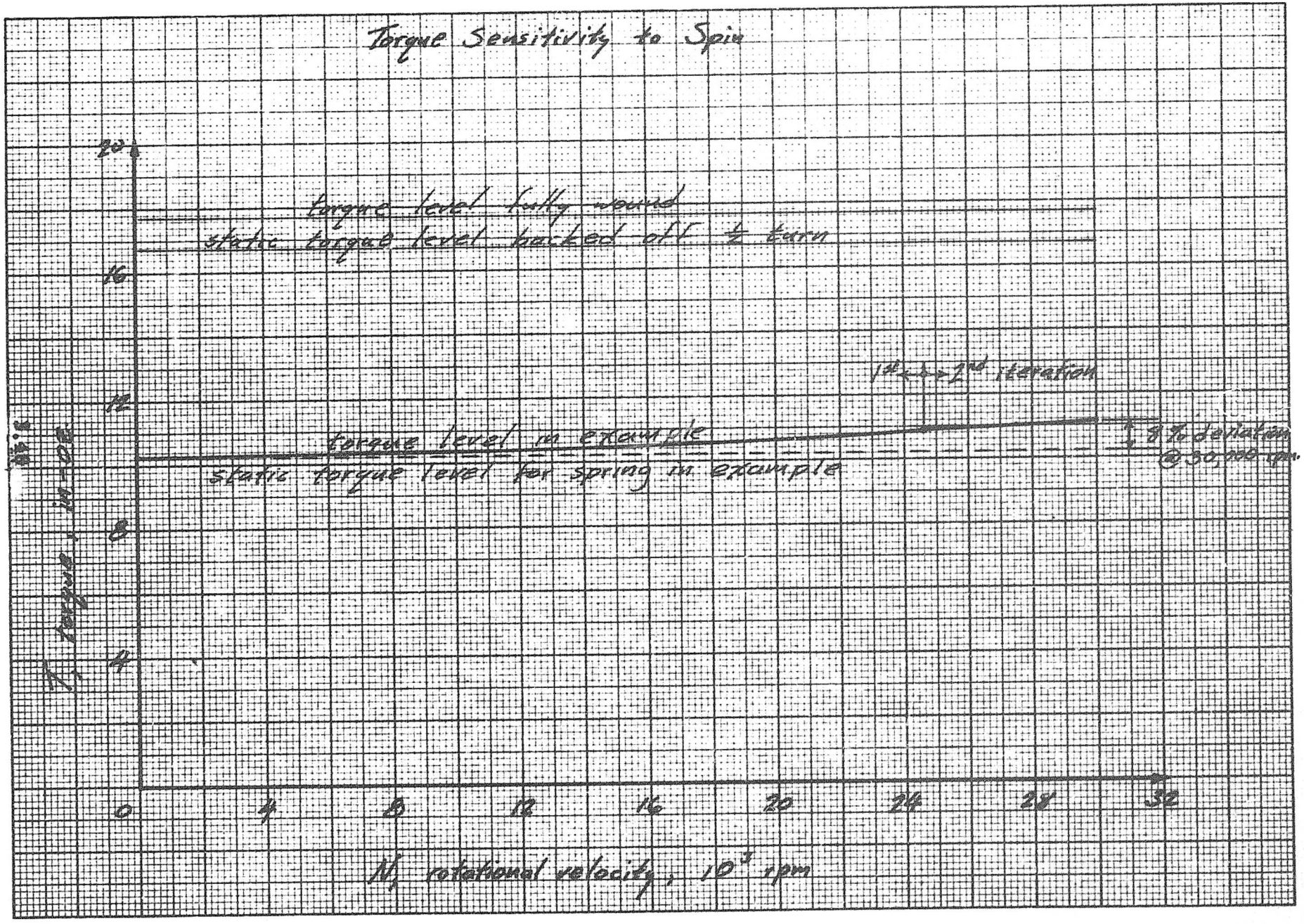

3.3.2 ECCENTRICITY OF DEFORMATION

3.3.2.1 Evidence of Occurrence of Eccentric Deformation

The possible importance of eccentric deformation of the motor spring was investigated by means of a preliminary test program. The results of these tests indicate the desirability of continuing an experimental program, as is presently under consideration.

The test which was run, was specifically designed to be in the range of large values of K, without regard for other parameters such as torque output, inner to outer radius ratio, length to thickness ratio, etc. No attempt is now being made to predict the range of parameters under which eccentric deformation may be expected. A full analysis will be the subject of later work.

The following photographs will indicate the nature of the eccentric behavior. Photograph (a) shows the non-spinning spring and (b) shows the same spring (under stroboscopic light) spinning at 1500 rpm. The direction of the motion of the main mass of spring with respect to the center arbor and the outer end (reference) was found to be well defined and repeatable. This direction was found to be very close to $\frac{\pi}{2}$ from the outer end, measuring in the direction of the spring length.

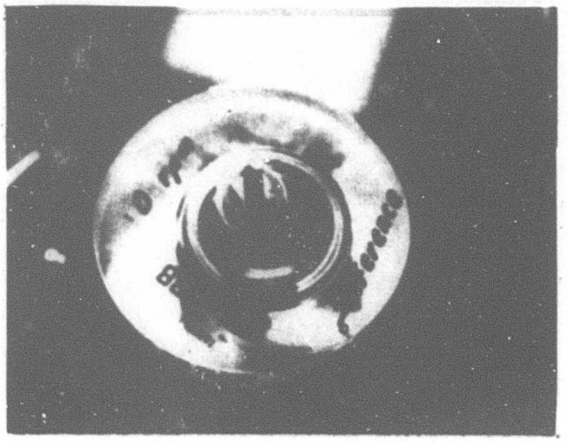

(a)

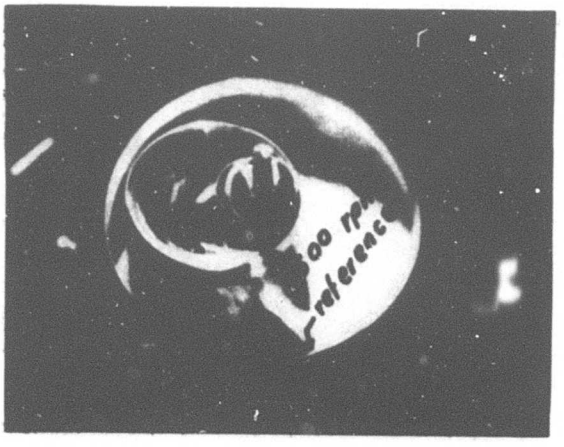

(b)

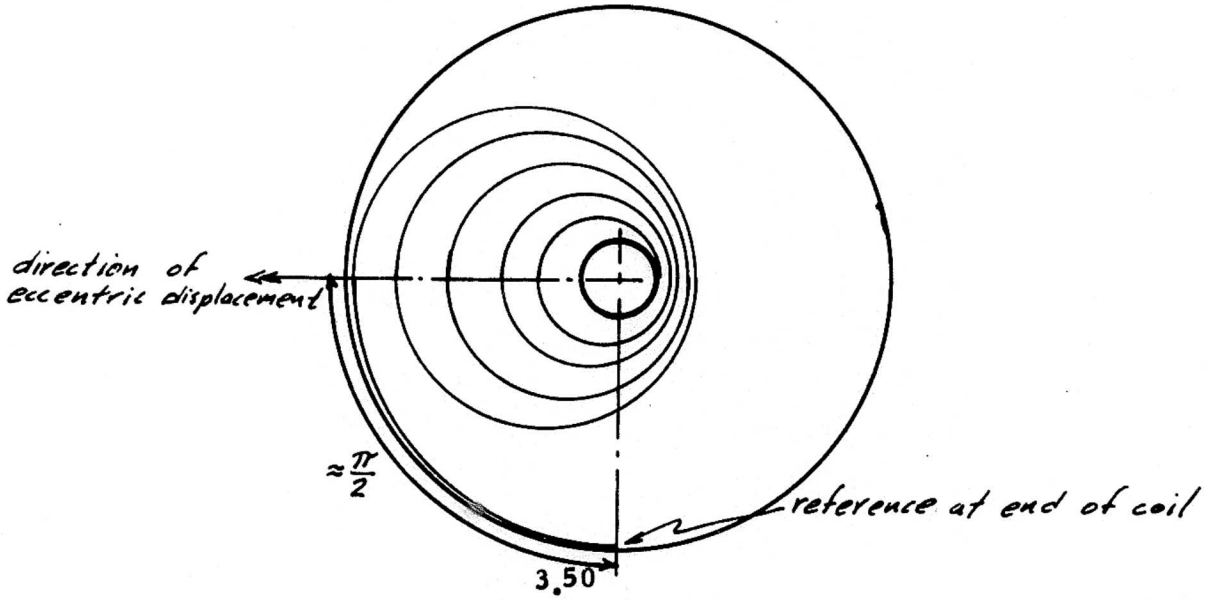
direction of
eccentric displacement
≈ π/2
reference at end of coil
3.50

Attempts to bias the stationary spring with eccentricity in a direction other than $\frac{\pi}{2}$, were difficult. The dash dot arc on the following photo shows the relative direction in which the biasing agents were forced from their original (broken line) orientation. The final eccentric spring orientation, for this case, was only slightly affected.

(c)

3.3.2.2 Eccentricity of Spiral Center of Gravity

The natural spring bias in the $\frac{\pi}{2}$ direction which is suggested by the foregoing (preliminary) test, may indicate the importance of the geometric eccentricity of the center of gravity of a spiral. This can be illustrated for a special case.

Assume that the spring forms a spiral of Archimedes, i.e., the radius is given by

$$r = r_0 - c\varphi$$

where

r_0 = outer (barrel radius

$2\pi c$ = spacing between coils (constant)

Then a parametric representation of the spring is

$$x = -r \sin \varphi$$
$$y = r \cos \varphi$$

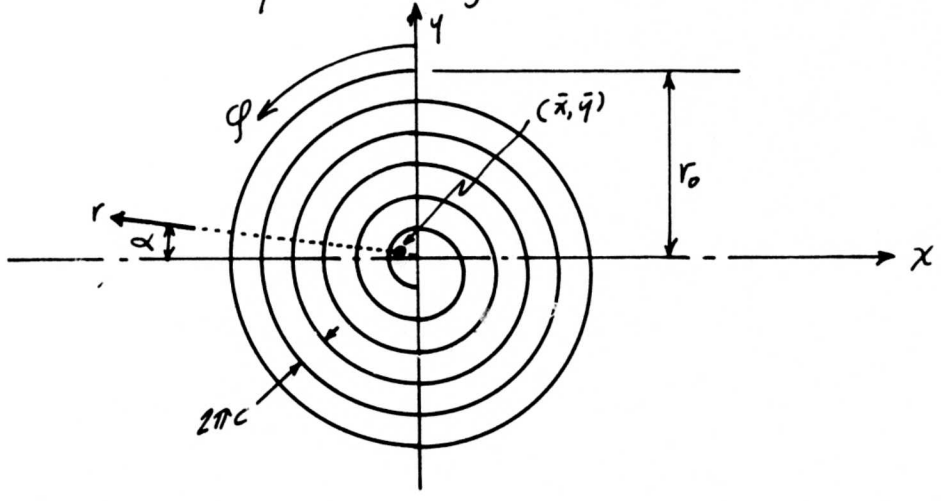

Let n number of coils (assumed an integral value for this discussion)

i.e., $\varphi_{max} = n 2\pi$

Then the center of gravity of the spring, $(\bar{x}, \bar{y})$ is given by

$$\bar{x} = \frac{\int x\,dl}{\int dl}$$

$$\bar{y} = \frac{\int y\,dl}{\int dl}$$

where dl = differential spring length = $r\,d\varphi$

The integrals are

$$\int dl = \int_0^{n2\pi} (r_0 - c\varphi)\,d\varphi = n2\pi(r_0 - nc\pi)$$

$$\int x\,dl = -\int_0^{n2\pi} (r_0 - c\varphi)\sin\varphi\,(r_0 - c\varphi)\,d\varphi = n2\pi c(-2r_0 + n2\pi c)$$

$$\int y\,dl = \int_0^{n2\pi} (r_0 - c\varphi)\cos\varphi\,(r_0 - c\varphi)\,d\varphi = 2n2\pi c^2$$

Thus $\bar{x} = -2c$

and $\bar{y} = 2c\,\frac{c}{(r_0 - nc\pi)}$

i.e., $\bar{x} = -\frac{\text{coil spacing}}{\pi}$

and the deviation of the c.g. $(\bar{x}, \bar{y})$ from $\varphi = \frac{\pi}{2}$ is given by

$$\alpha = \tan^{-1}\left|\frac{\bar{y}}{\bar{x}}\right| = \tan^{-1}\left|\frac{c}{r_0 - nc\pi}\right|$$

This is a small angle for most spring configurations, indicating that the eccentricity is located approximately at

$$\left(\varphi = \frac{\pi}{2}\,,\ r = -\bar{x} = 2c\right).$$

3.3.2.3 Generalization of "Axi-Symmetric Bending Analysis

In the energy analysis of the axi-symmetric bending deformation, it was implicitly assumed that the deformed shape of the coils remained circular, as in the initial idealization. Furthermore the initial idealization was assumed axi-symmetric. This analysis can be generalized as follows:

(a) Allow r to be a continuous function of ϑ rather than discrete values r_i, thereby changing the sum on i to an integral on $d\vartheta$;

(b) Decrease the range of each K_j, thereby changing the sum on j to an integral on dK (or on $d\omega$);

(c) Allow the initial idealization to be eccentric and allow the deformed shape to be eccentric and non-circular.

For the present, the implications of (c) will be considered in a preliminary manner, since this direction of analysis shows the greatest promise for the investigation of eccentric deformation. Initially the center of the undeformed (circular) coils should be displaced from the center of the arbor (which is the center of spin).

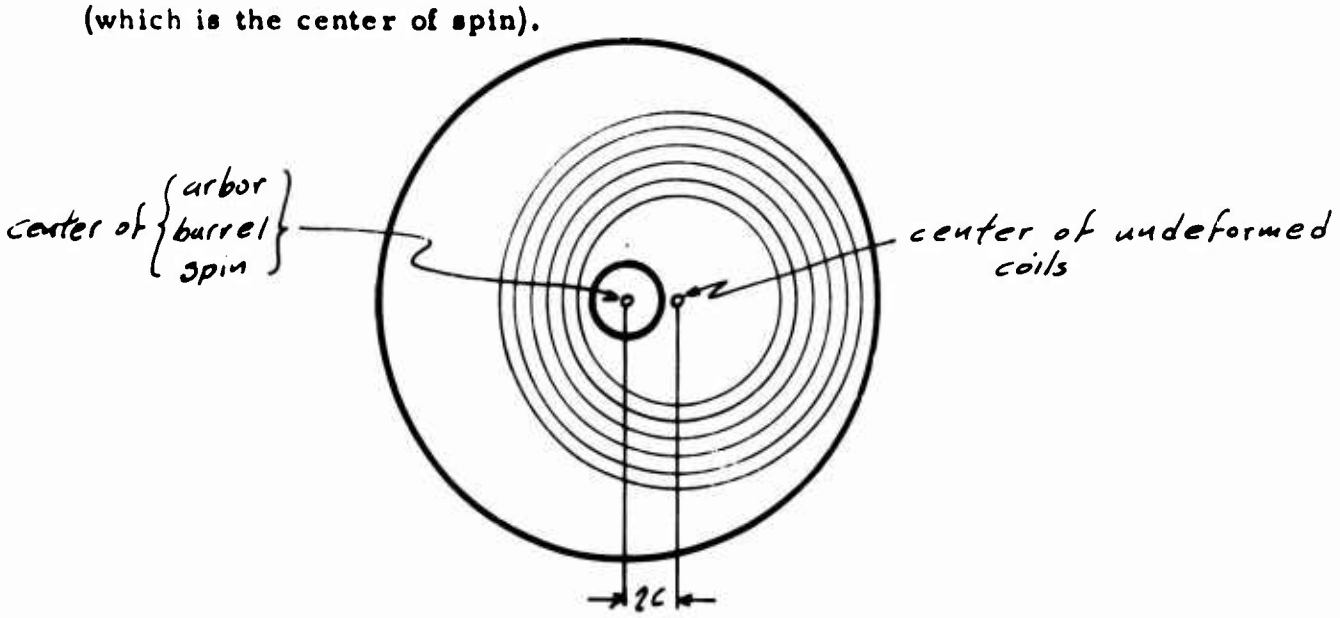

3.54

The deformed spring coils must be allowed to displace as well as deform (still within the confines of the arbor-barrel constraints).

For this purpose the initial radius can be expressed

$$r_i \left(1 + \frac{2c}{r_i} \cos \vartheta\right)$$

which assures that the initial eccentricity is equal to $2c$ (see section 3.2.3). Then rather than a constant deformation u_i ; around the circumference, a rigid body rotation plus a constant deformation plus an elongation of the circle is allowed.

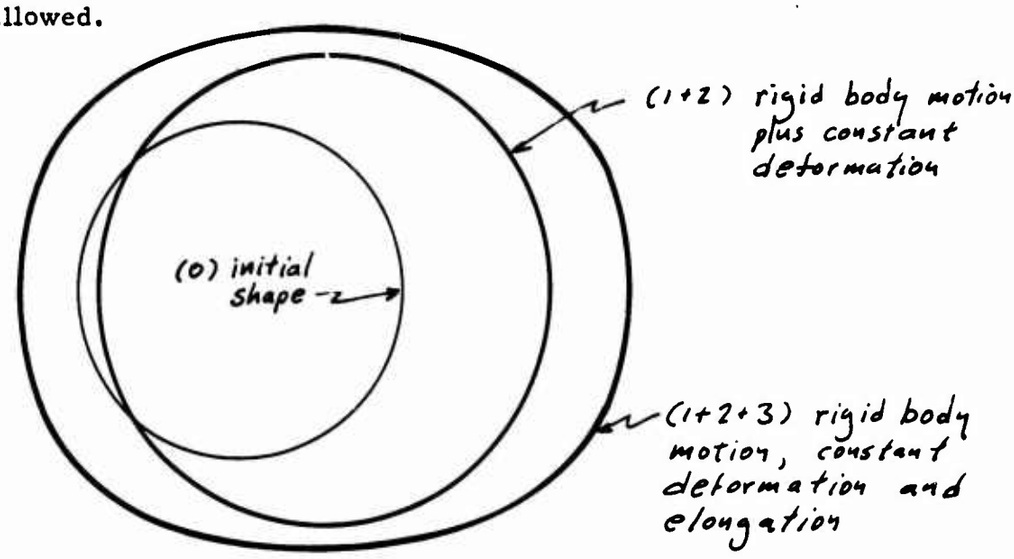

This deformation is expressable in harmonics of a Fourier expansion:

$$u_i = [R + D \cos \vartheta + E \cos 2\vartheta]$$

R: radial growth of circle; $D \cos \vartheta$: rigid body displacement; $E \cos 2\vartheta$: elongation of shape

The potential function Π must be minimized with respect to the parameters R_i, D_i and E_i now, rather than merely u_i. i.e., in

functional notation:

$$W = W(R_i, D_i, E_i)$$
$$U = U(R_i, D_i, E_i)$$
$$\Pi = U - W = \Pi(R_i, D_i, E_i)$$

$$\frac{\partial \Pi}{\partial R_i} = 0 \quad , \quad \frac{\partial \Pi}{\partial D_i} = 0 \quad , \quad \frac{\partial \Pi}{\partial E_i} = 0 \ .$$

The constant length condition, analogous to its previous form, is only concerned with radial <u>growth</u>, R_i. The parameters D_i and E_i which indicate coil <u>position</u> and coil <u>shape</u>, do not influence the spring length. Thus the constant length condition appears as:

$$\sum_{i=1}^{n} R_i = 0 \ ,$$

which supplies the n^{th} equation in R, where $n-1$ equations are supplied by $\frac{\partial \Pi}{\partial R_i} = 0$ (as in the case of U_i, section 3.1.2.3). The equations $\frac{\partial \Pi}{\partial D_i} = 0$ and $\frac{\partial \Pi}{\partial E_i} = 0$, hold for all values of i including $i = n$; thus yielding a set of $3n$ equations for R_i, D_i and E_i.

3.3.2.4 <u>Effect of Eccentric Deformation on Torque</u>

<u>The important thing about the inner coil with regard to spring torque position is its radius of curvature at its point of attachment with the arbor</u>. In the case of eccentric deformation, the possibility of periodic fluctuations of the spring output torque becomes evident since the radius of curvature of the spring at its arbor interface, is determined by the direction of the spring eccentricity. It appears at this time, that the direction of the eccentricity does not bear a constant relationship to the orientation of the arbor-spring connection; but instead varies as the spring unwinds.

In preceding sections, it was found that the direction of the initial spiral eccentricity (and, based on this, of the final eccentricity) is approximately 90° from the outer end connection; for the special case of a spring in the shape of a spiral of Archimedes, having an integral number of coils. It would be of interest to inquire into the position of the initial eccentricity for the case of an arbitrary (not necessarily integral) number of coils, as well as the non-Archimedian spiral configurations. This would be an impor. nt part of the investigation along with the extension and modification of the present axi-symmetric solution.

As was pointed out in section 3.2.3, the spiral's initial eccentricity can be accounted for by including additional terms in the expansion of the axi-symmetric spring deformation expression. These terms, in addition to allowing for initial (non-spinning) coil eccentricity, will provide for eccentric coil deformation. i.e., in the axi-symmetric case, only radial coil growth was considered, whereas in this case coil elongation and rigid body coil motion are possible.

In order to obtain an estimate of the possible result of eccentric coil deformation, an illustrative example will be presented.

Assume that an arbor and the first coil of a spiral spring may be idealized as shown below,

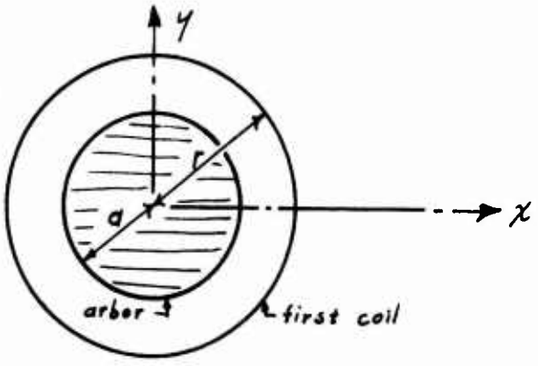

Then, letting the above schematic represent the axi-symmetric case for a particular configuration, the illustrative problem will consist of the determination of the effect of non-circularity of the first coil, which would result from non-axi-symmetric deformation.

To this end a simple assumed deformed shape will be considered in order to avoid obscuring the meaning of the results of this illustrative example with premature complexity. (The results of this example will thus represent an order-of-magnitude indication of the possible extent to which eccentricities can affect spring torque output.) The assumed shape will be that of an ellipse,

(a) the circumferential length is taken equal to that of the first circular coil; so that only deformations without extensions are being considered.

(b) the minor axis is the same length as the diameter of the arbor.

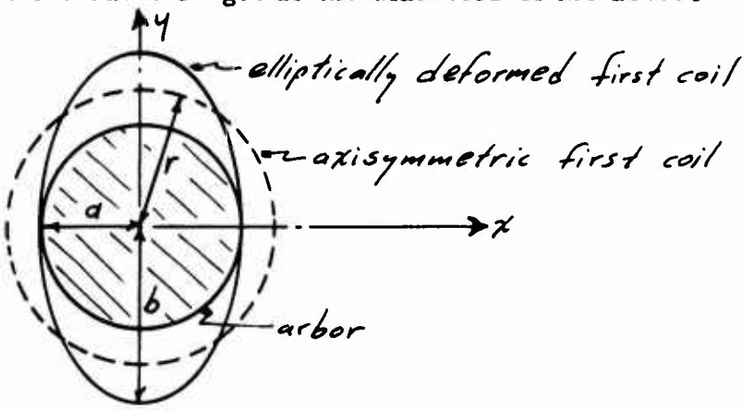

Thus, to be explicit, the symbols in the above figure represent:

r = first coil radius when circular (axi-symmetric)

a = arbor radius = semi-minor axis of elliptical first coil shap (with coil length unchanged)

b = semi-major axis of elliptical first coil shape

The length of the semi-major axis, b , under these two conditions ((a) and (b)), can be shown to be approximated by the following expression in terms of axi-symmetric configuration, i.e., arbor radius, a, and circular first coild radius, r :

$$b = a\left(1 - \frac{\pi}{2}\right) + r\,\frac{\pi}{2} \qquad (1)$$

The equation of the ellipse shown on the preceding sketch is

$$\frac{x^2}{a^2} + \frac{y^2}{b^2} = 1$$

Thus the radius of curvature at any point may be found to be given by

$$\rho = \frac{(a^4 y^2 + b^4 x^2)^{3/2}}{a^4 b^4} \qquad (2)$$

At the points of maximum and minimum curvature this becomes:

$$\left.\begin{aligned} \rho\,(0,b) &= a^2/b \\ \text{and} \quad \rho\,(a,0) &= b^2/a \end{aligned}\right\} \qquad (3)$$

Using the same numerical values as were used in the previously mentioned report (TR #64-11), take

$$a = .11"$$

$$r = .12"$$

$$EI = .375\ \#\ in^2$$

which corresponds to the spring in the example examined in that report, rotating at 34,300 rpm.

Thus, from (1) and (3), one finds:

$$b = .1257$$

$$\rho(0,b) = .0962$$

$$\rho(a,0) = .1435$$

Then the change in moment at these same points, from that of the coil in its circular (i.e., non-eccentric) position, is given by :

$$\left.\frac{\Delta M}{EI}\right|_{(0,b)} = \frac{1}{\rho(0,b)} - \frac{1}{r} = 2.06 \ in^{-1}$$

$$-\left.\frac{\Delta M}{EI}\right|_{(a,0)} = \frac{1}{r} - \frac{1}{\rho(a,0)} = 1.37 \ in^{-1}$$

This means that the first coil, if it remained circular, would impose a constant torque producing moment, M, upon the arbor. However, that same coil, if it had an elliptical shape imposed upon it by the eccentricity of its deformation, could impose moments which vary from the value M by the preceding ΔM values. Thus with $EI = .375$, as stated previously, the imposed torque could vary from

$$M_{max} = M_{Symmetric} + 12.36 \ \text{in.-oz.}$$

to

$$M_{min} = M_{Symmetric} - 8.22 \ \text{in.-oz.}$$

depending on the relative arbor-first coil orientation (where M, at this spin rate, for the example is approximately 11.4 in-oz).

Then assuming that the position of the arbor relative to the first coil varies continuously around the circumference during a single turn of the arbor in the unwinding cycle, the resultant torque characteristic appears as shown on the following curve.

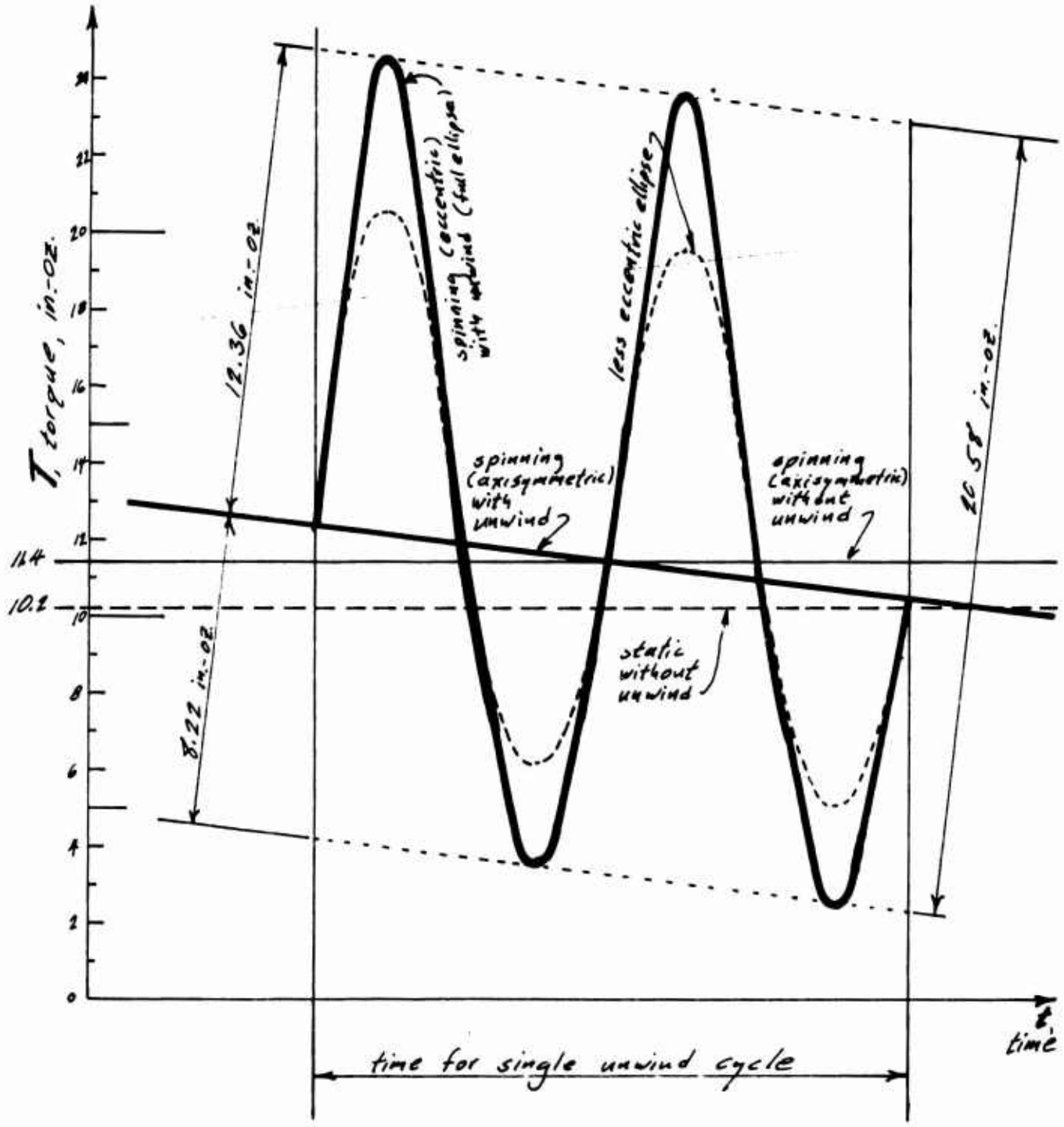

Spiral Spring Torque Characteristic in Spin Environment

Eccentric Deformation

3.4. SUMMARY OF RESULTS

(a) For the non-spinning spring in a barrel:

$$T = T_{max} - \frac{EI}{l} k \, (\varphi_{max} - \varphi)$$

where

T = spring torque at any value φ

φ = angle through which spring has been turned

φ_{max} = angle turned to reach "solid spring" state

EI = spring section stiffness

l = spring length

$k = \begin{cases} 1 \\ 1.25 \end{cases}$ fixed end at barrel / pinned end at barrel

$$T_{max} = \begin{cases} b\sigma_y \left[\left(\frac{h}{2}\right)^2 - \frac{1}{3} \left(\rho \frac{\sigma_y}{E}\right)^2 \right] k_1 , & \rho < \rho_{min} \\ b\sigma_y \frac{h^2}{6} k_1 , & \rho = \rho_{min} \\ k_1 \frac{E}{\rho} \frac{bh^3}{12} , & \rho > \rho_{min} \end{cases}$$

b, h = width and thickness of spring section

σ_y, E = yield stress and modulus of elasticity of spring

ρ = arbor radius

$\rho_{min} = \frac{E}{\sigma_y} \frac{h}{2}$

(b) Additional torque in spinning spring, due to extensional deformation only (membrane):

$$T_N = m \omega^2 r^2 \quad , \varphi \neq 0 \; ; \; \varphi < \varphi_{max}$$

where

m = mass per unit length of spring

ω = spin rate

$r = \rho$ = arbor radius

(c) Maximum bending torque in spinning spring is given by radius of curvature of spring at arbor, as in static case

$$T = T_{max} \text{ (of (a) above)}$$

(d) Change in bending moment in spinning spring is determined by means of the relationship:

$$\Delta M = EI \frac{u_1}{r^2}$$

where

u_1 = radial deformation of first coil

r = coil radius $\approx$ constant

and

$$u_1 = -K \frac{\sum_{i=2}^{n} R_i^3 (R_i^2 - 1)}{1 - \sum_{i=2}^{n} R_i^3}$$

and

$$\Delta T = k_1 \Delta M$$

In the event that the coils "bottom-up" the iterative procedure to obtain described in this report is utilized.

4. PIVOT AND JOURNAL FRICTION

Technik has found that torque losses associated with pivots and journals are attributable to a complex set of phenomena, of which the "conventional" definition of "friction" provides only one portion. Thus the analysis which was performed, and is described herein, serves to point up the additional work necessary for the full understanding and description of the phenomena involved.

The analysis which is presented here is the conventional "Hertzian" elastic contact deformation analysis. For the purpose of generating quantitative information, this analysis is combined with a torque evaluation based on an assumed coefficient of friction, although the value to be assigned to such a coefficient is greatly dependent upon the nature of the physical interference phenomenon involved.

4.1 ELASTIC ANALYSIS

For the present, although various geometries differ (i.e., journals and pivots) and may require somewhat different treatment, the pivot will be examined in order to expose certain basic problem areas. Consider a spherical pivot point in a spherical seat, as shown below:

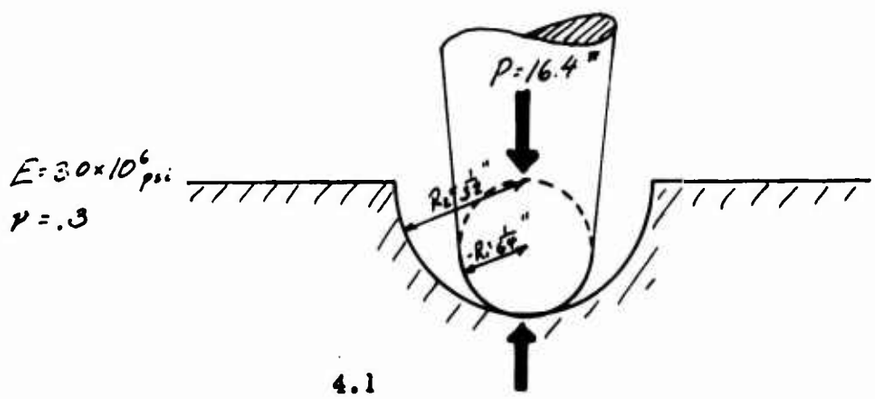

Then from Hertzian theory, the radius of interface pivot-seat contact is

$$a = 1.109 \sqrt{\frac{P}{E}\left(\frac{R_1 R_2}{R_1 + R_2}\right)} = 2.86 \times 10^{-3}"$$

and the maximum interface pressure, q_o, is given by

$$q_o = \frac{3P}{2\pi a^2} = .97 \times 10^6 \text{ psi}$$

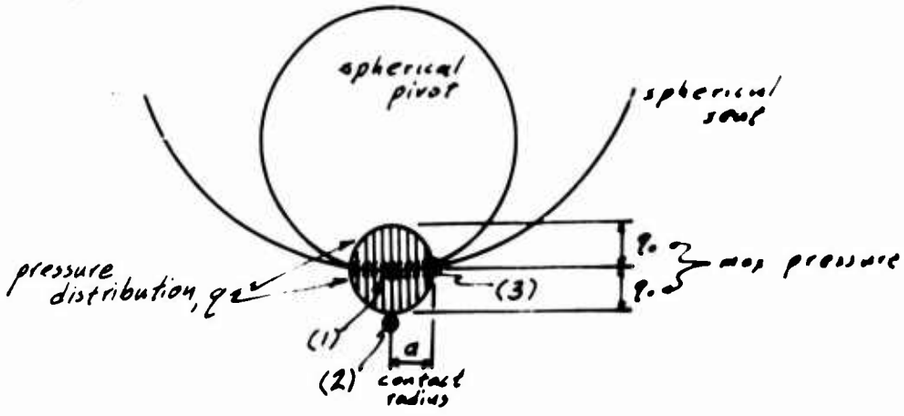

The stresses at the points (1,2,3) shown above, may be shown to give rise to the maximum shear stresses (for Tresca yield criterion);

$$\tau_{(1)_{max}} = .1\, q_o = 97{,}000 \text{ psi}$$

$$\tau_{(2)_{max}} = .3\, q_o = 299{,}000 \text{ psi}$$

$$\tau_{(3)_{max}} = .13\, q_o \; (= \sigma_{(3)}) = 126{,}000 \text{ psi}$$

Note that the maximum shear stress at the center of the circle of contact (1) is $.1\, q_o$, whereas the normal stress is q_o. For the ductile materials being considered, the maximum shear stress is a good indicator of

the incidence of plastic action. This value must be compared to shear yield (τ_y) which can be taken to be $\frac{\sigma_y}{2}$; σ_y = tensile yield of the material.

Thus, for many hardened steels used for pivots, the stress at point (1) does not indicate plastic action while the stress at (3) is probably of a marginal nature in this respect. The stress, $\tau_{(2)_{max}}$, at (2), however, indicates a plastic zone below the surface of the spherical seat. It is questionable at this time, without further investigation, whether this zone extends to the surface (at (3)). If it does not, the plastic zone will be elastically contained and should not be accompanied by large deformations.

If, on the other hand, the zone reaches the surface to become unconfined, large deformations may accompany the action, with resulting large frictional areas and associated torques.

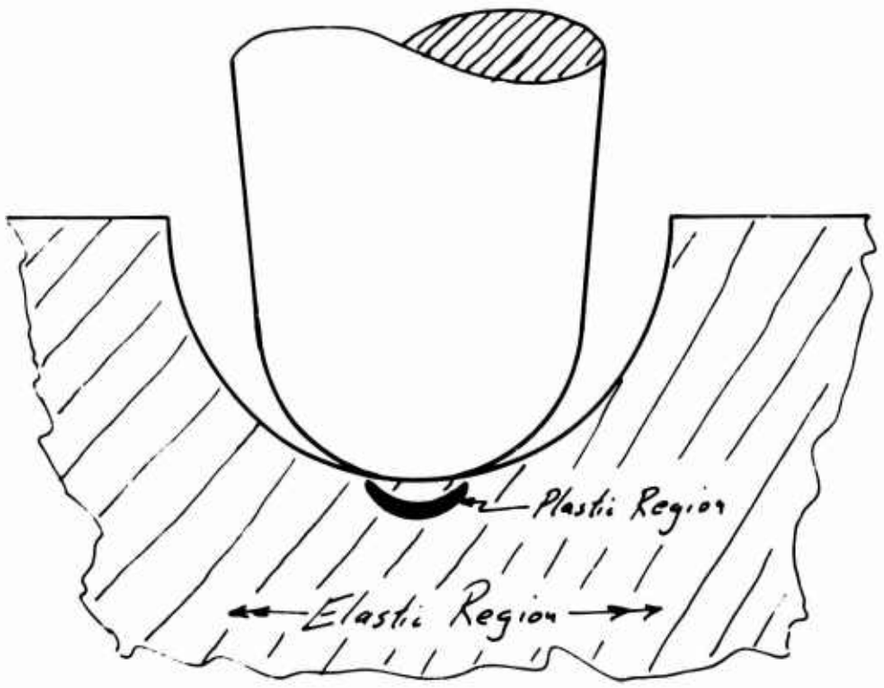

4.2 TORQUES IN ELASTIC CASE

The pressure distribution between the spherical pivot and seat for the elastic (Hertzian)analysis, is;

$$q = q_0 \left[1 - \left(\frac{r}{a}\right)^2\right]^{\frac{1}{2}}$$

thus the torque is given by

$$T = \int_0^a r(\mu q \, dA)$$

Taking μ constant

$$T = \frac{\pi^2}{8} q_0 a^3 \mu$$

Thus for $a = 2.86 \times 10^{-3}$ (16.4# load)

$$T = 27 \mu \times 10^{-3} \text{ in.-lb}$$

or

$$T = .17 \mu \text{ in.-oz}$$

It may thus be noted that the torque T, lost at the pivot is directly dependent upon the value of μ, the coefficient of friction. A frequently encountered value of this coefficient is (say) $\mu = .3$. In this case

$$T = .051 \text{ in.-oz.} \qquad (\mu = .3)$$

and values of μ may be found, as great as, or even greater than, unity (seizing). The actual limit on attainable values of μ is imposed by the shearing strength of the material.

If, in general, the frictional force, μq, at any point exceeds the shearing stress of the material, the material will, in fact, shear; resulting

in a greatly accelerated wear process. The process will continue, always causing the pivot and seat to conform to each other and increasing the contact radius, until the friction force, μq, no longer exceeds the shear strength at any point. Thus, the contact radius having been increased, the frictional torque losses will likewise increase.

To visualize the accelerated wear process, assume the following highly idealized rotating pivot-seat configuration, i.e., conical and flat, respectively:

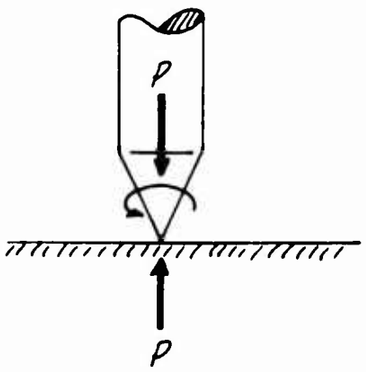

The initial pressure, q, at the point of contact approaches infinity, thus for any value of μ, $\mu q > \tau_o$, where τ_o is a constant, ie., that value of shear stress which will cause the material to shear. As the material shears the cone is truncated and the seat is simultaneously "worn" so that a finite contact radius, a, is attained:

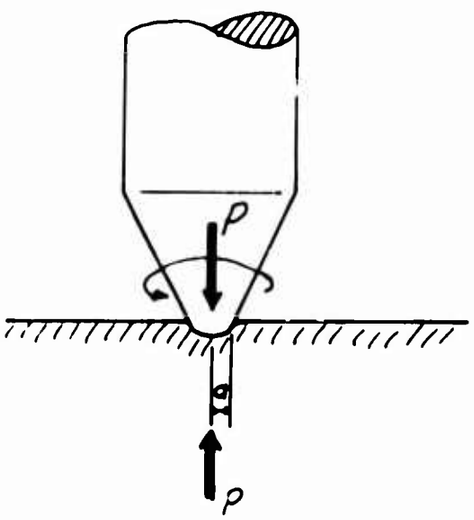

Thus the interface pressure reduces as a increases, until the value of μq at no point exceeds τ_0 ; since, if this value is exceeded, shearing will occur changing the pressure distribution, q , increasing the contact radius a , and reducing μq below the τ_0 value. At this time "accelerated wear" is considered to cease and the more conventional wear ensues.

Thus the question of torque losses rather than encompassing only considerations of geometry, material and "friction" linked by elastic analysis should be broadened. Included in the investigation should be the additional analyses concerned with

(a) plastic deformation of contacting parts - increase in contact area and friction losses over elastic case;

(b) accelerated wear process - shearing of material and associated friction torque increase.

5. BEAM HAIR SPRING PROBLEMS

An outline of preliminary results of two hair spring problems investigated by Technik will be presented in the following pages.

5.1 EFFECT OF SETBACK ON HAIR SPRING

Statement: Given the beam shown below, find the maximum "g" loading that it can support. Establish general criteria as well as specific results for the general range of dimensions presented.

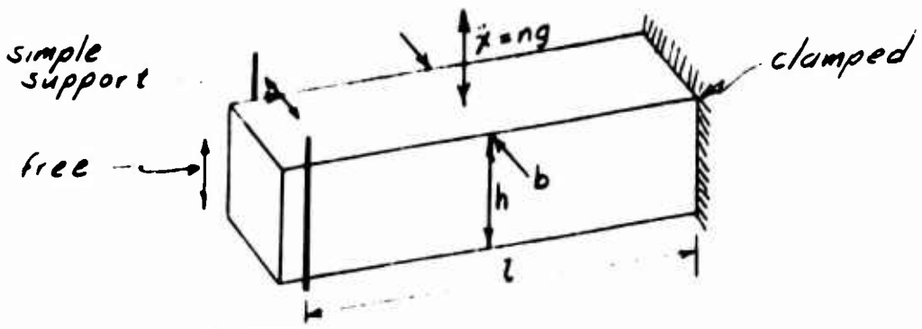

Ranges

b = .00330 - .00008 (in)

h = .013 - .001 (in)

E = 25×10^6 (# /in^2)

ν = .3

ρ = .3 (#/in^3)

$.3 \leq l \leq .45$ (in)

$200 \times 10^3 \leq \sigma_{yp} \leq 250 \times 10^3$ (#/in^2)

$8{,}000 \leq n \leq 25{,}000$ (desired)

In the solution of this problem we will at first assume that there is no initial warping of the spring; further work under the scope of the proposed task will remove this restriction.

Remarks: The following analysis indicates that the limitation on the capacity of the hair spring to resist set back forces may be provided by its plastic deformation rather than its buckling configuration. Further investigation must determine the more "exact" limits of the two phenomena.

Approach: The solution was approached by two techniques; both of which assumed the existence of a buckling configuration, and then by different approaches derived their basic equations. In the first a differential equation approach was formulated through the use of the elastic equations for bending and twisting of simple beam configurations. This resulted in three equations, two of which were coupled in their first-order effects. The eigen-values of this coupled pair of equations, subject to the correct boundary conditions, provides the critical load. Unfortunately because the resultant equation was highly non-linear its solution was considered beyond the scope of this exploratory activity.

In the second approach an integral-equation formulation was obtained through the use of energy techniques. Although exact solutions are again difficult, this approach lends itself to approximate solutions. The assumption of one variable, subject to all the displacement boundary conditions, allows the complete integration and a reduction to an algebraic form; from which the critical load can be obtained. Although this is simpler than the differential equation approach, it is quite laborious.

A third alternative presents itself for the solution of this problem; that of bounding the correct solution by others which are presently known. Although this technique is limited if precise values of the critical "g" loading are required, as would be necessitated in optimum design; it is of real value in the solution to the present problem. The bounding problems utilized were the uniformly-loaded and end-loaded cantilever beam, and the uniformly-loaded simply-supported and clamped beams.

In addition to the limitations imposed by the "bounding" solutions another limitation presents itself, and must be considered in all problems of this type; plastic deformation of the beams. It is found that this often provides a lower limit on the "g" loading, over and beyond the possibility of lateral buckling; unless the beam is optimum designed to avoid this type of limitation.

The accompanying figure presents a curve of "n" (ng's) which the spring can withstand as a function of beam length; all other dimensions are as specified on the cross-section. From this it is seen that plastic flow is a real limitation in this problem, and that the lateral buckling rigidity is more than adequate; even though only a lower bound on this rigidity is calculated. In the interpretation of this limit, based on the initiation of plastic flow, it is important to note that a yield stress of 200×10^3 to 250×10^3 psi was assumed; which may be beyond that which the material can develop. In the latter event the "n" curve

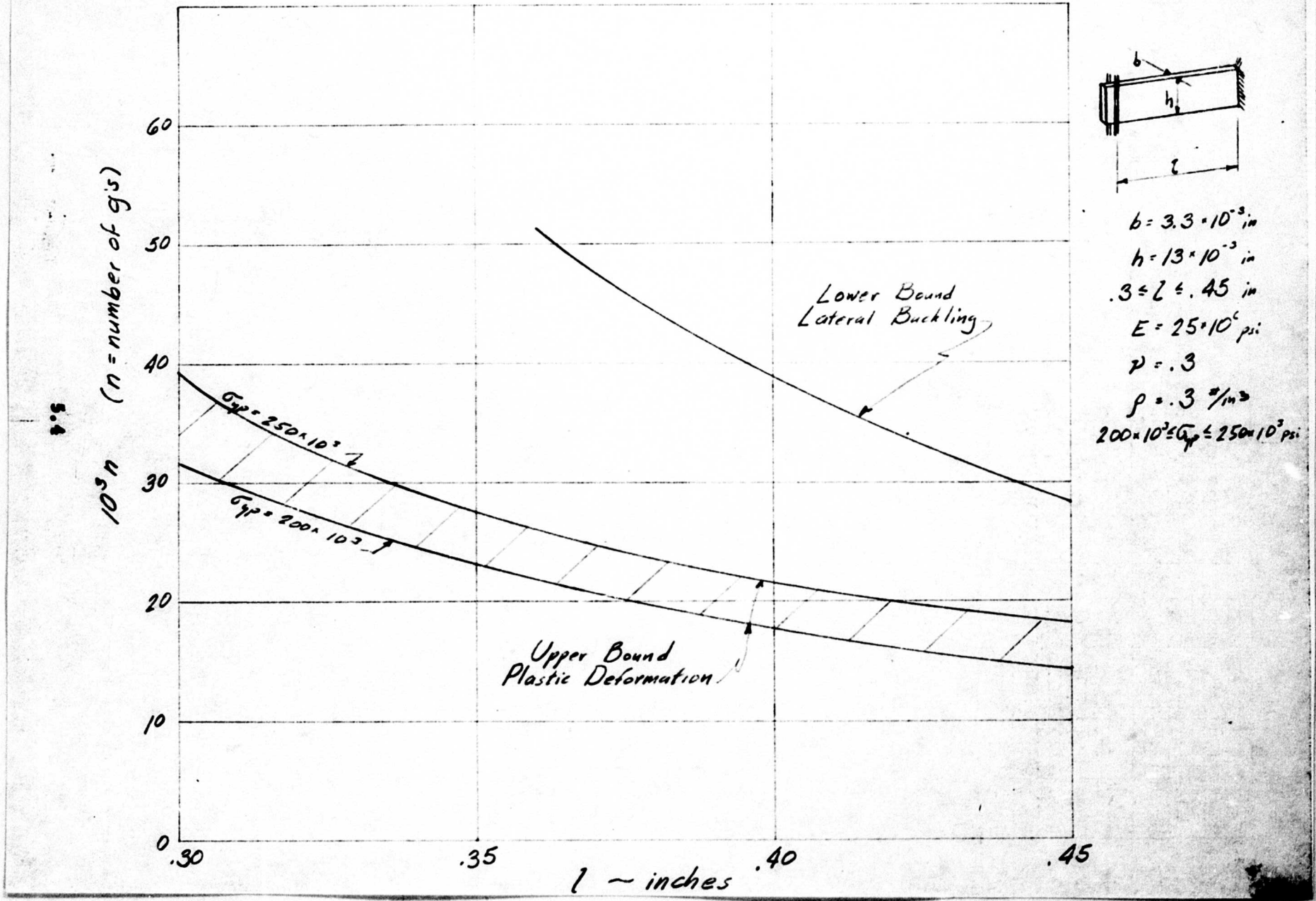
$10^3 n$ (n = number of g's)
60
50
40
30
20
10
0
.30
.35
.40
.45
l ~ inches
Lower Bound
Lateral Buckling
Upper Bound
Plastic Deformation
$\sigma_{yp} = 250 \times 10^3$
$\sigma_{yp} = 200 \times 10^3$
b
h
l
$b = 3.3 \times 10^{-3}$ in
$h = 13 \times 10^{-3}$ in
$.3 \leq l \leq .45$ in
$E = 25 \times 10^6$ psi
$\nu = .3$
$\rho = .3$ #/in³
$200 \times 10^3 \leq \sigma_{yp} \leq 250 \times 10^3$ psi

would be suitably lowered. An optimum design of this beam would raise the plastic curve with little, if any, drop of the buckling curve, subject to little or no weight increase; thereby substantially increasing the load carrying capacity of the beam-like member. Further work in these directions could be expected to result in a definitive evaluation of beam hair spring design.

5.2 EFFECT OF A WEDGE RETAINER ON HAIR SPRING

Statement: Investigate the effects upon the bending characteristics of the same beam as was described in Problem #1, of an imposed curvature at the fixed end.

Background: The function of the beam is to perform as a spring resisting an applied torque as illustrated below:

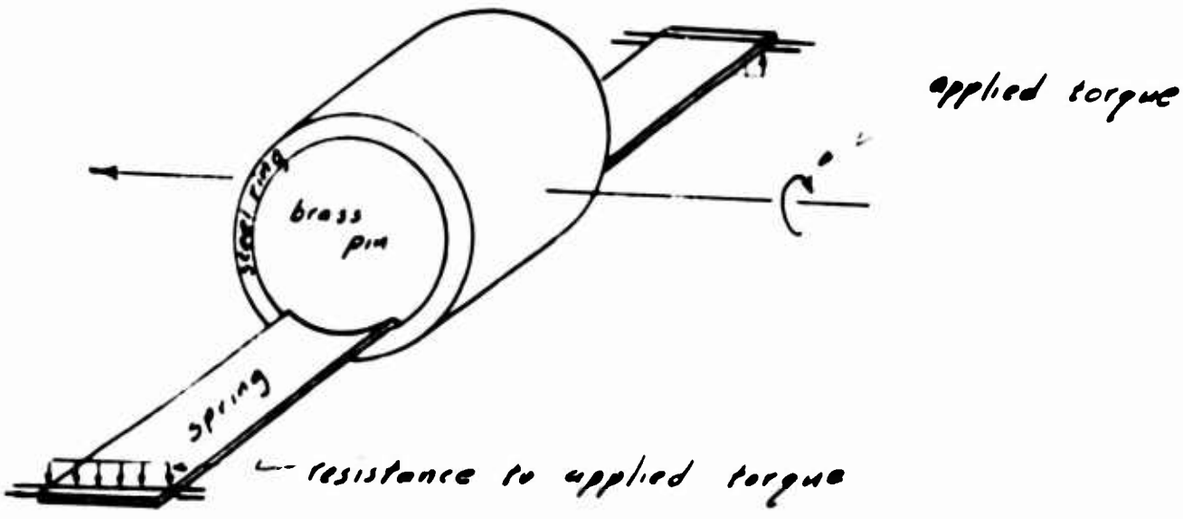

The bending characteristics of the above spring are influenced by an initial curvature imposed on a portion of the spring during the fabrication of the above assembly. The extent of the deviation of these bending characteristics from those of the hitherto employed idealization (i.e., a flat strip) has been

questioned. This discussion is, therefore, directed toward discerning that extent.

Remarks: The following approach indicates that the presence of the wedge retainer (in that it deforms the hair spring) greatly changes the bending characteristics of the hair spring from those of an assumed "flat" hair spring. A more "exact" evaluation of these changes awaits further investigation and will be undertaken under the scope of the present proposed task.

Approach:

Phase a: Extent of Deformation at Fixed End

Assuming that the insertion of the brass pin and the spring into the steel ring causes no practical change in the curvature of the steel ring, then the surface of the fuze spring in contact with the steel ring will take on the ring curvature.

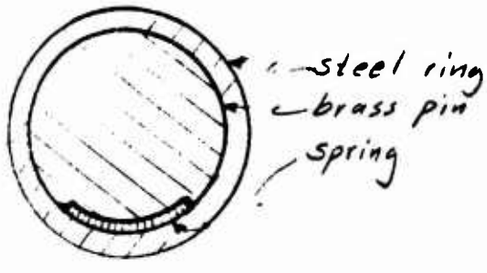

The maximum relative transverse deflection (sag) thus imposed on the spring is equal to the relative deflection between the edges of the spring and the center of the spring.

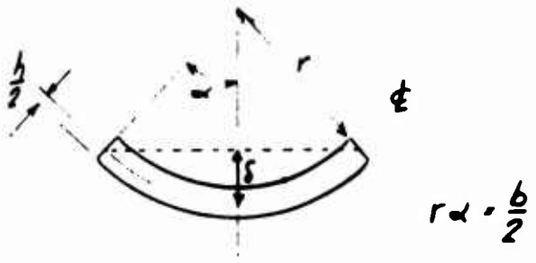

Actually this "sag", δ , can vary with the tolerances on the ring and on the fuze spring itself; a representative value, however, was found to be quite large.

Phase b: Effect of an Assumed Distribution of the Deformation

In the initial stages of this investigation, it was assumed that the angle α was small. This can be shown to lead to incorrect results and the analysis must be revised to account for α being large. This revision is reflected in the reported Phase a above, and Phase c below. For Phase b only, the original assumption of α small, will still be assumed to hold, thus providing a lower bound on the effects of the curvature (i.e., the small α assumption yields a smaller value for the curvature than the value subsequently found).

Under the above condition, and assuming St. Venant's principal concerning the extent of the influence of an edge disturbance, it was theorized that a parameter describing the effect of the deformation might be the number of widths thru which the deformation might be equivalently assumed to hold in an undiminished state.

A number of curves are presented based on that investigation.

These curves show the deflection of the end of the spring for a load, $\mathfrak{E}p$ (at that end) considering spring lengths of .3" to .45". It was assumed that the actual deflection of the spring would fall somewhere between that of the spring with an undiminished cylindrical deformation extending one width (b) and the spring with an undiminished cylindrical deformation extending three widths (3b). (Note: the remainder of the spring was assumed flat).

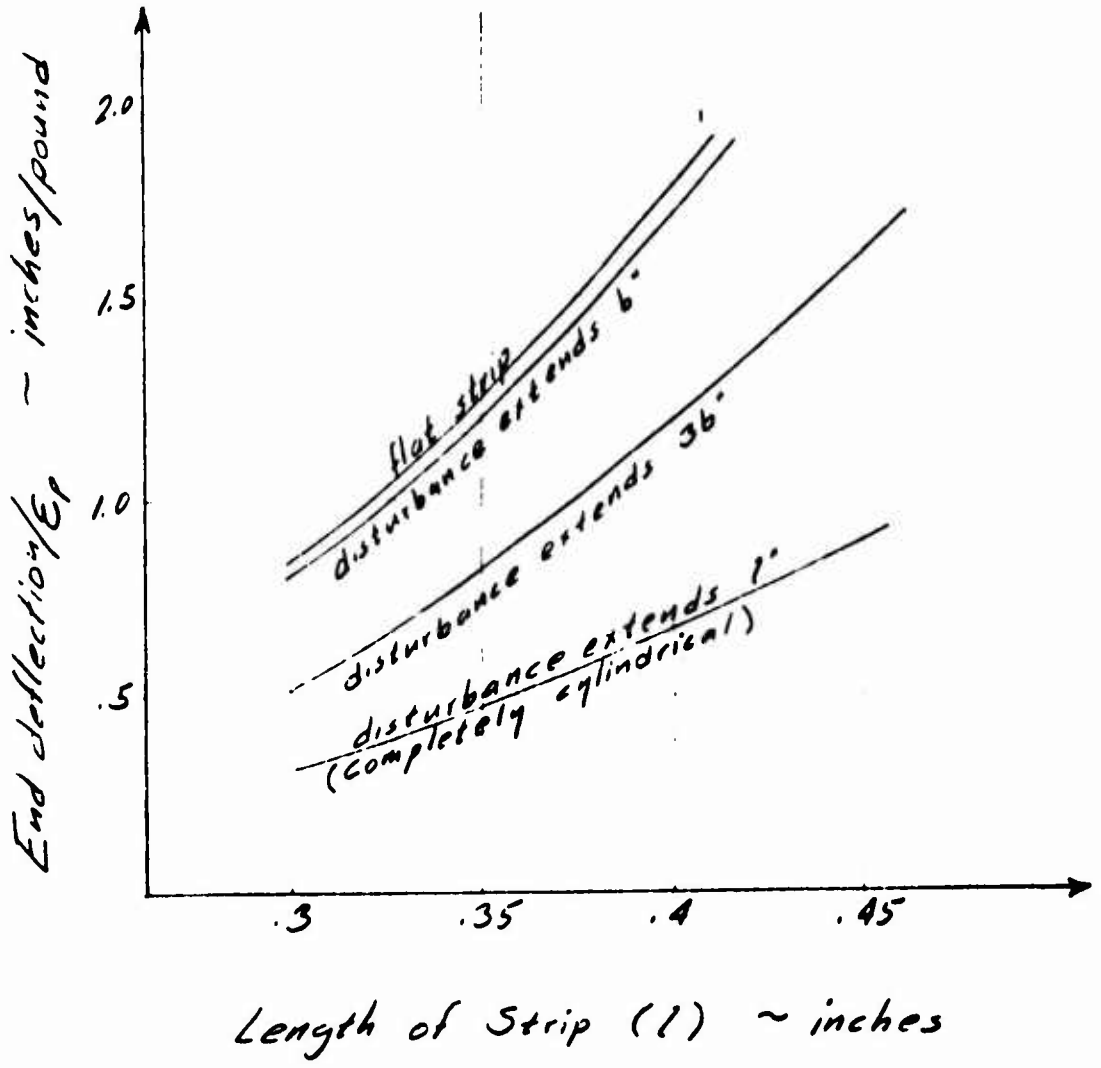

In view of the shortcomings of the assumption upon which these curves are based, they are presented merely for an appreciation of the possible magnitude of the deviation of bending characteristics of the deformed spring from those of the flat spring idealization. As was pointed out previously, the actual deviation would be expected to be greater than that shown.

Phase c: Determination of the actual extent of the deformation caused by an initially imposed curvature at the fixed end of the spring.

The revised maximum deflection (Phase a) was found to be non-trivial. Since this deflection falls into the large deflection category (i.e., $\delta > h$), no conclusion can be drawn as to the local character of the deformation and, for this reason, an estimate of the actual extent of the deformation was undertaken.

The spring was treated as a flat plate subjected to loading conditions so distributed as to bend the plate to the required configuration; but to have no resultant force transverse to the plate.

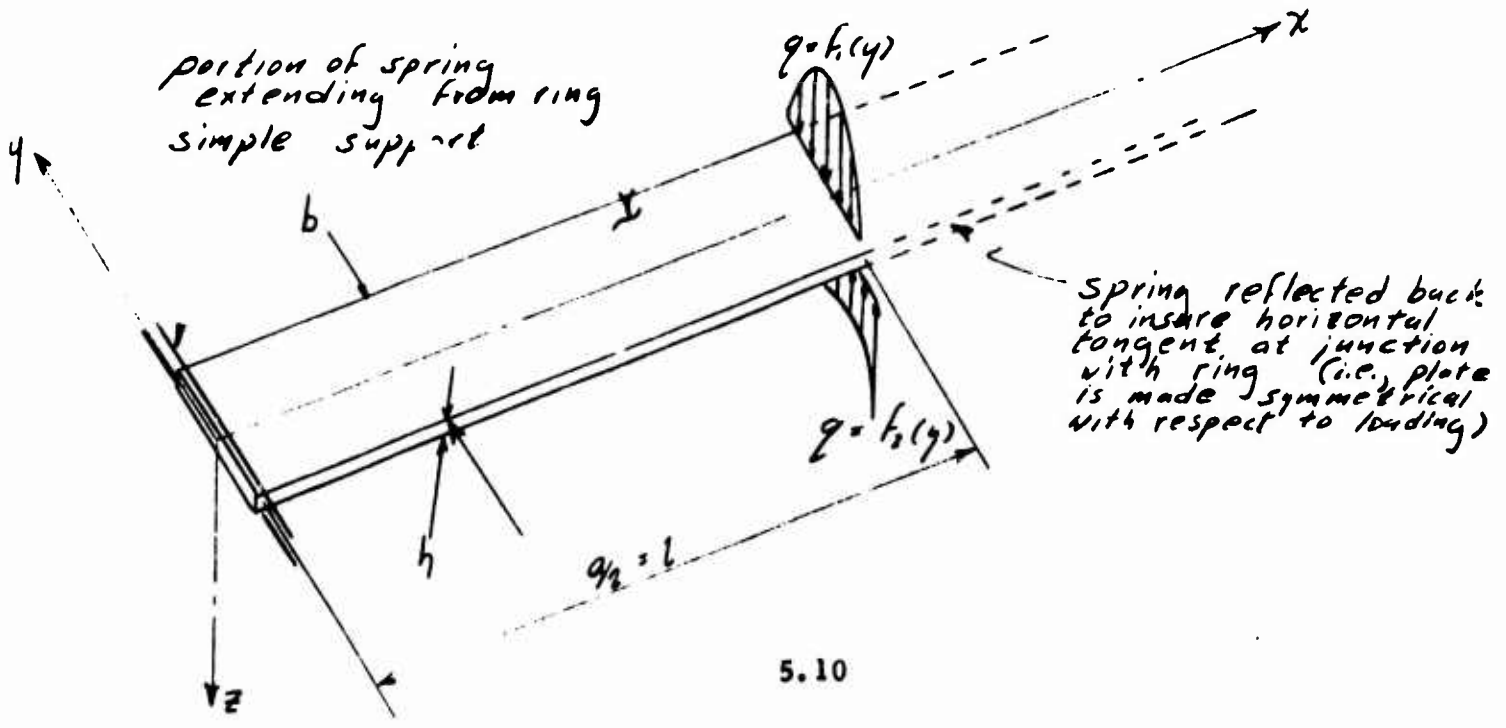

Based on this an infinite series expansion was found for the deflection of the spring in the z direction. The following curves show this deformation when either one or two terms of the series are employed. The series converges so rapidly that addition of the third term would not be warranted.

A number of factors are evident from inspection of the curves:

(1) The spring retains some portion of the initially imposed curvature over its entire length.

(2) The curvature in the y direction gives rise to a curvature in the x direction.

It appears that the former assumption of a local deformation associated with the end effect requires much further justification. The determination of the bending characteristics of the spring in its presently conceived configuration (as shown in the curves using first and second terms of the series) is complex. The procedure would hold only if the yield stress of the spring were not exceeded. The local relaxation resulting from such excessive stresses, would result in an attenuation of the cylindrical end effect, i.e., the spring would act more like a flat plate or beam.

Approximation of Deflection Curve of Hair Spring Due to Deformation Imposed on End

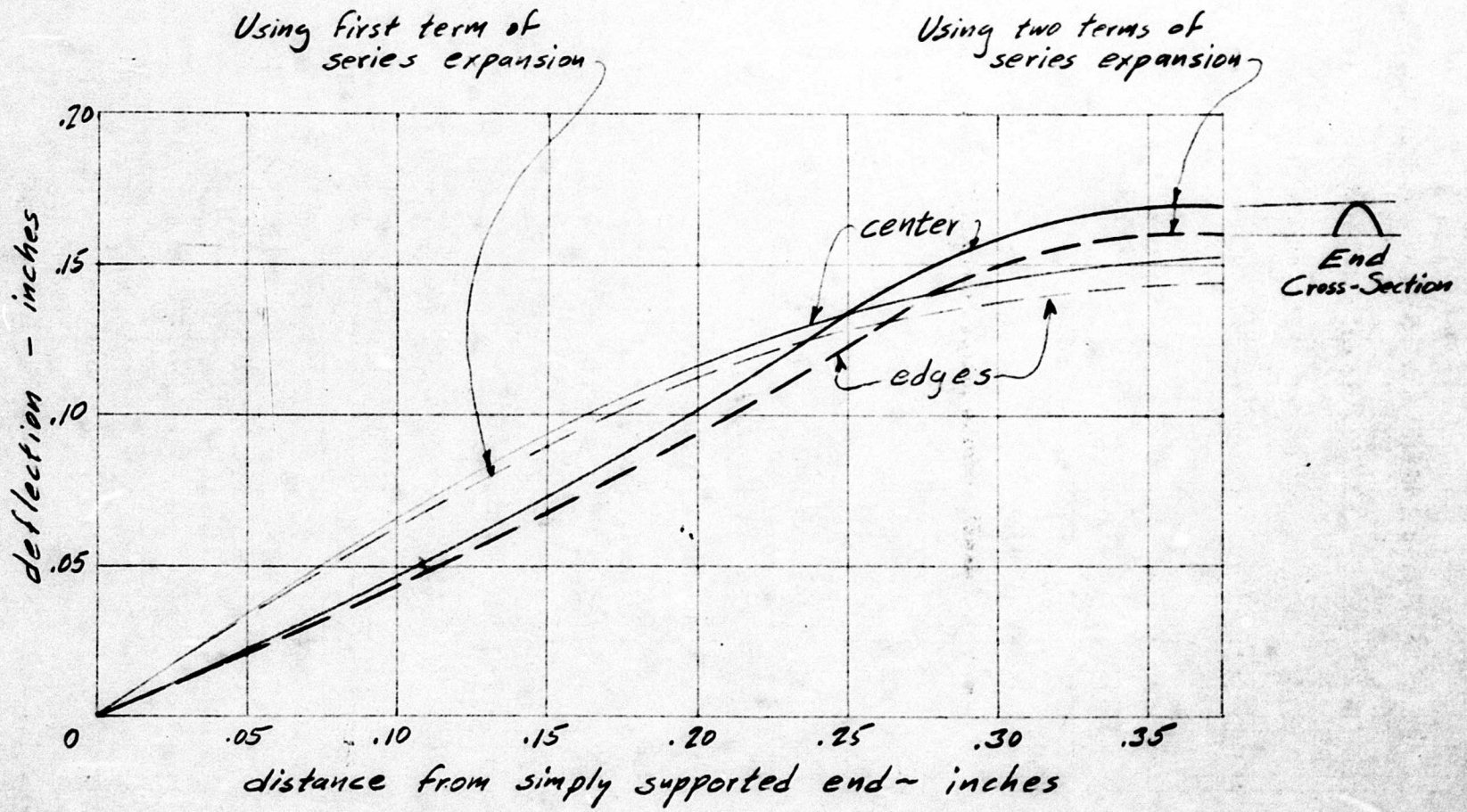

6. TORSION HAIR SPRING

Torsion hair springs are often subject to the same phenomena associated with rotating shafts, i.e., resonance at critical speeds. This resonance consists of the coincidence of the spin rate of the projectile (and therefore, of the hair spring) with one of the modes of transverse bending vibration of the hair spring. Thus the values of those spin rates which correspond to critical speeds of the torsion hair spring, are dependent upon the properties and configuration of that hair spring.

The ultimate purpose of the hair spring, which is concerned with its time keeping characteristics, is to oscillate in its torsional mode. For this reason, the design of the spring is based upon the objective of obtaining a specific natural frequency of the spring acting in concert with a rotary inertia. The attainment of this natural frequency is dependent upon the same properties and configuration considerations as are the values of the critical speed spin rates.

Thus, one finds an interrelationship which exists between the primary, time keeping, characteristic of the torsion hair spring and the secondary, critical speed, characteristic which constitutes possible degradation of the functioning capability of the time keeping system.

In order to illustrate this relationship, the following specific case will be investigated.

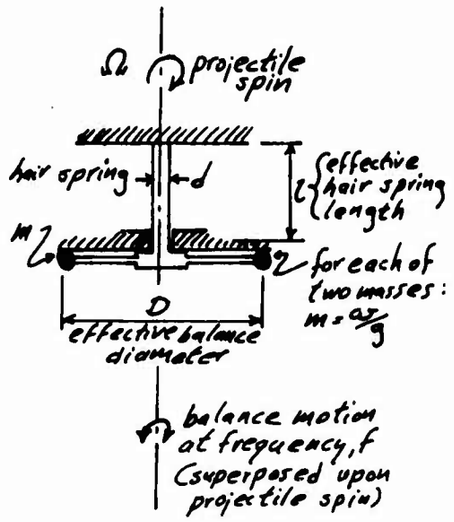

6.1 TORSIONAL FREQUENCY (f)

The balance oscillates in a torsional vibration about the centerline, superposed on the overall projectile spin, Ω . The frequency, f , of this oscillation can be shown to be given by:

$$f = \frac{\sqrt{2.36}}{2\pi} \times 10^3 \frac{d^2}{\sqrt{m D^2 \ell}}$$

for a steel wire (modulus of elasticity, E = 30x10^6 psi and Poisson's ratio, ν = .3), where

f = natural frequency in torsional mode (cps)

d = spring diameter, circular section (in)

m = concentrated mass $\approx$ 1/2 total balance mass

D = effective diameter between masses, m. (in)

ℓ = effective length of hair spring (in)

6.2 "WHIRL" FREQUENCY (Ω_{crit})

Likewise, it can be shown that for the special case where the rotary inertia of the end is constrained so that the shaft can be considered fixed-fixed, the critical speed, Ω_{crit}, is given by

$$\Omega_{crit} = 49{,}100 \frac{60}{2\pi} \frac{a_i d}{l^2}$$

for steel again, where

$a_i = a_1, a_2, \cdots$ = discrete constants, the value of which depends on the mode shape (of the bending vibration).

$a_1 = 22.0$

$a_2 = 61.7$

$a_3 = 121.0$

APPENDIX A: CURVED BEAM ENERGY EXPRESSIONS

For a curved beam, as shown below, it can be shown that for a non-extensional bending deformation

$$\frac{M}{EI} = \left(\frac{1}{R} - \frac{1}{R_1}\right)$$

where $R_1 = R + \Delta R$

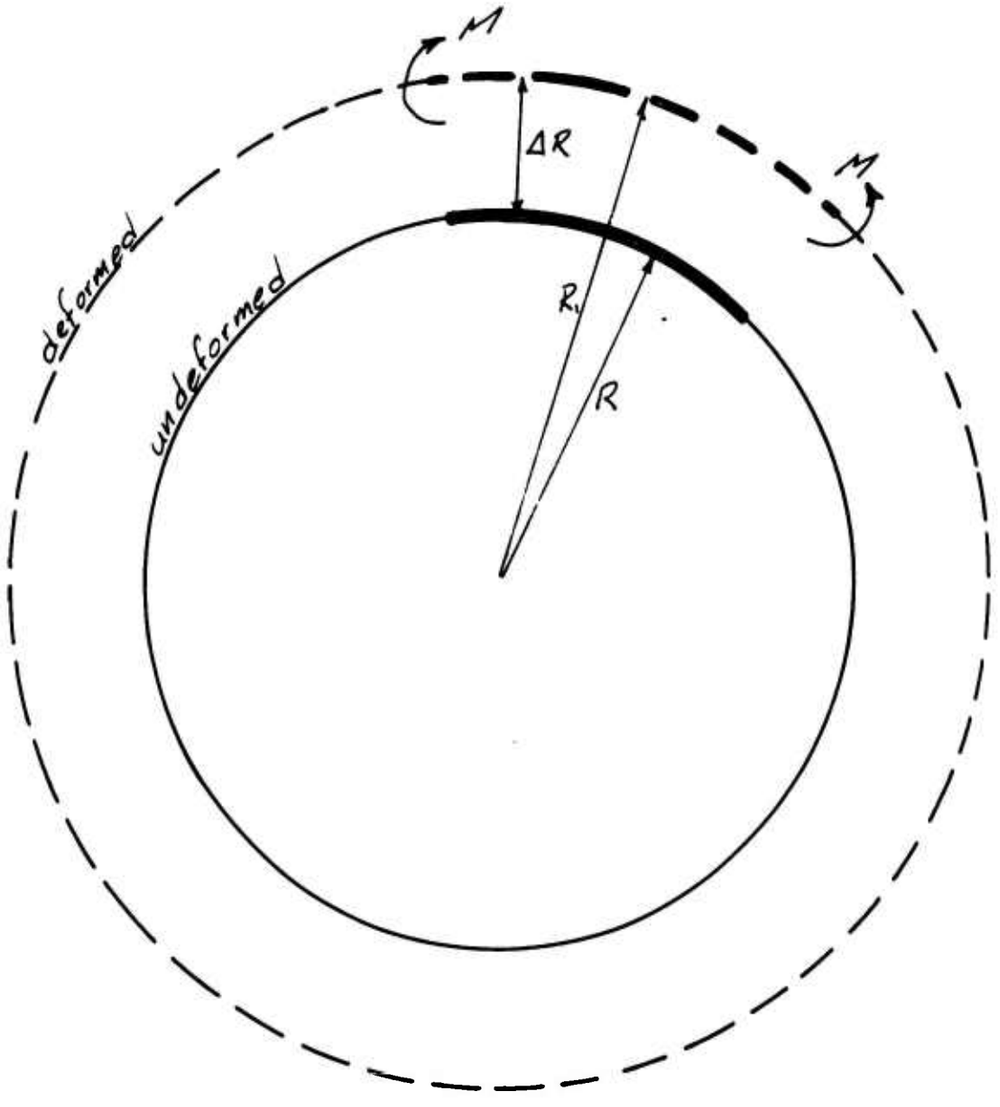

Combining these two equations, one finds

$$M = EI \frac{\Delta R}{R(R+\Delta R)}$$

For small bending deformations of a full coil $\Delta \ell = u$, this can be linearized as:

$$M = EI \frac{u}{R^2}$$

Thus the strain energy of the full coil is given by

$$U = \frac{1}{2EI} \oint M^2 ds$$

$$U = \pi EI \frac{u^2}{R^3}$$

The work done by centrifugal forces in moving the coil element through the displacement, u, is given by

$$W = \int_0^{2\pi} \int_R^{R+u} \underbrace{\underbrace{\{(m r d\vartheta)}_{d(\text{mass})} \omega^2 r\}}_{d(\text{force})} dr$$

$d(\text{work})$

which for a full coil becomes,

$$W = 2\pi \omega^2 m \left[R^2 u + R u^2 + \frac{u^3}{3} \right]$$

Again, for small deformations, u, this can be linearized as:

$$W = 2\pi \omega^2 m R^2 u$$

APPENDIX B: FIRST ITERATION FOR SECTION 3.3.1.2.3.1

$$u_1 = -K\left[\frac{\sum_{i=1}^{n} R_i^3 (R_i^2 - 1)}{1 + \sum_{i=1}^{n} R_i^3}\right] \qquad \text{(based on } s,01 \text{ approximation)}$$

$$u_1 = K\left[R_1^3(R_1^2 - 1) + R_1^3\left(\frac{u_1}{K}\right)\right], \quad R_i = \frac{r_i}{r_n} = \frac{r_i}{r_1}$$

r_i	R_i	R_i^2	R_i^3	$R_i^2 - 1$	$R_i^3(R_i^2-1)$	$\frac{u_1}{K} R_i^3$	$\frac{u_1}{K}$	$\frac{u_1 r_1^5}{K} \cdot 10^3$
.125	1	-	-	-	-	-	-4.65*	-.142 **
.150	1.2	1.44	1.728	.44	.76	-8.04	- 7.28	-.222
.175	1.4	1.98	2.74	.98	2.68	-12.7	-10.	-.306
.200	1.6	2.56	4.09	1.56	6.37	-19.0	-12.36	-.378
.225	1.8	3.24	5.82	2.24	13.	-27.1	-14.1	-.431
.250	2.0	4.00	8.0	3.00	24.	-37.2	-13.2	-.404
.275	2.2	4.84	10.6	3.84	40.80	-49.3	-8.5	-.260
.300	2.4	5.78	13.9	4.78	66.50	-64.6	1.9	.058
.325	2.6	6.78	17.6	5.78	101.80	-81.9	19.9	.61
.350	2.8	7.82	21.9	6.82	149.00	-102.	47.	1.44
Σ			86.38		404.91			0 ***

$$u_1 = -K\left[\frac{404.91}{87.38}\right]$$

$$u_1 = -4.65K \qquad \leftarrow *$$

$$u_1 = -.142 \times 10^{-3}\left(\frac{K}{r_1^5}\right) \qquad \leftarrow **$$

*** "Constant length" condition